INFORMATION TO USERS

This was produced from a copy of a document sent to us for microfilming. While the most advanced technological means to photograph and reproduce this document have been used, the quality is heavily dependent upon the quality of the material submitted.

The following explanation of techniques is provided to help you understand markings or notations which may appear on this reproduction.

1. The sign or "target" for pages apparently lacking from the document photographed is "Missing Page(s)". If it was possible to obtain the missing page(s) or section, they are spliced into the film along with adjacent pages. This may have necessitated cutting through an image and duplicating adjacent pages to assure you of complete continuity.

2. When an image on the film is obliterated with a round black mark it is an indication that the film inspector noticed either blurred copy because of movement during exposure, or duplicate copy. Unless we meant to delete copyrighted materials that should not have been filmed, you will find a good image of the page in the adjacent frame.

3. When a map, drawing or chart, etc., is part of the material being photographed the photographer has followed a definite method in "sectioning" the material. It is customary to begin filming at the upper left hand corner of a large sheet and to continue from left to right in equal sections with small overlaps. If necessary, sectioning is continued again—beginning below the first row and continuing on until complete.

4. For any illustrations that cannot be reproduced satisfactorily by xerography, photographic prints can be purchased at additional cost and tipped into your xerographic copy. Requests can be made to our Dissertations Customer Services Department.

5. Some pages in any document may have indistinct print. In all cases we have filmed the best available copy.

University
Microfilms
International

300 N. ZEEB ROAD, ANN ARBOR, MI 48106
18 BEDFORD ROW, LONDON WC1R 4EJ, ENGLAND

LEGRANGE, JANE DEBORAH

HIGH RESOLUTION HEAT CAPACITY STUDIES NEAR THE NEMATIC-SMECTIC A PHASE TRANSITION

University of Illinois at Urbana-Champaign PH.D. 1980

HIGH RESOLUTION HEAT CAPACITY STUDIES NEAR THE NEMATIC-SMECTIC A PHASE TRANSITION

BY

JANE DEBORAH LEGRANGE

B.A., University of Pennsylvania, 1975
M.S., University of Illinois, 1977

THESIS

Submitted in partial fulfillment of the requirements
for the degree of Doctor of Philosophy in Physics
in the Graduate College of the
University of Illinois at Urbana-Champaign, 1980

Urbana, Illinois

UNIVERSITY OF ILLINOIS AT URBANA-CHAMPAIGN

THE GRADUATE COLLEGE

June, 1980

WE HEREBY RECOMMEND THAT THE THESIS BY

JANE DEBORAH LEGRANGE

ENTITLED HIGH RESOLUTION HEAT CAPACITY STUDIES NEAR THE NEMATIC-SMECTIC A PHASE TRANSITION

BE ACCEPTED IN PARTIAL FULFILLMENT OF THE REQUIREMENTS FOR THE DEGREE OF DOCTOR OF PHILOSOPHY

Jack W. Mockel
Director of Thesis Research

R. O. Simmons
Head of Department

Committee on Final Examination†

Jack W. Mockel
Chairman

Robert Joseph Maurer

Ursula E. Kruse

E. Atlee Jackson

† Required for doctor's degree but not for master's.

O-517

ACKNOWLEDGMENTS

The author wishes to thank

Professor Jack M. Mochel, her advisor, for valuable technical assistance, friendship, and encouragement;

Dr. Mark Sears for his help with data fitting;

Professor William Pirkle for his advice on chemical analysis;

Dr. P. E. Cladis and Professor D. L. Johnson for providing samples;

Professor Don Ginsberg for his role as surrogate advisor during Jack Mochel's sabbatical leave;

the members of her research group and other graduate students, who lived in the basement, for interaction on research matters, as well as friendship, and a lot of laughs;

Doron for all the delicious meals he cooked and constant moral support.

This thesis is dedicated to her father and to the memory of her mother who have always been a source of strength and friendship.

This research was supported in part by NSF Grants DMR 76-01058 and DMR 77-23999.

"Liquid crystals are beautiful and mysterious; I am fond of them for both reasons."

P. G. deGennes

TABLE OF CONTENTS

CHAPTER 1

INTRODUCTION

Liquid crystals are long, asymmetric organic molecules which do not show a single transition from solid to liquid, but exhibit a variety of phases whose symmetries and mechanical properties are intermediate between those of a liquid and a crystal. These phases are defined by the orientational and spatial ordering of the molecules and can change as a function of temperature (thermotropic liquid crystals) or of concentration of the rodlike molecules in solvent (lyotropic liquid crystals).

Liquid crystal molecules are typically 25 Å long and 5 Å wide. Aromatic rings and adjacent double bond linkages form a rigid core while the alkyl end chains are flexible. The chemical structures of four liquid crystals and the sequence of phases for each are shown in Figure 1.

The nematic phase is characterized by long range orientational order where the molecules are aligned along a preferred direction called the director, $\hat{n}$, and $+\hat{n}$ and $-\hat{n}$ are physically equivalent. There is no order in the positions of the centers of mass. The molecules are free to rotate about their long axes and there is no average dipole moment. The system is optically uniaxial with the optical axis parallel to the director.

In the smectic phases, known as A, B, and C, the molecules are stacked in two dimensional layers. Within each layer there is high orientational order with the molecules aligned along a preferred direction.

Smectics A and C are known as disordered smectics, which can be visualized as stackings of two dimensional liquids. There is no long range

Figure 1. The chemical structure and sequence of phases for the compounds studied.

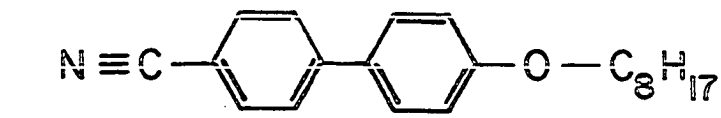

C ⟷ S_A ⟷ N ⟷ I

octyloxycyanobiphenyl (8OCB)

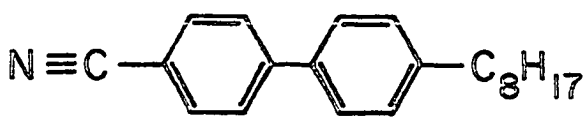

C ⟷ S_A ⟷ N ⟷ I

octylcyanobiphenyl (8CB)

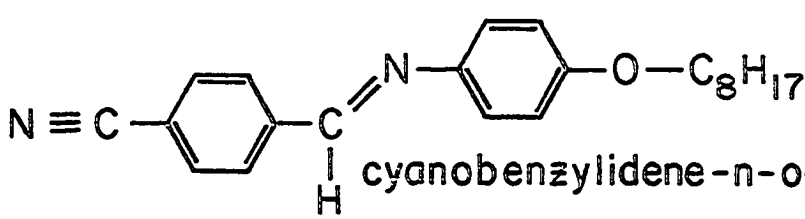

cyanobenzylidene-n-octyloxyaniline (CBOOA)

C ⟷ S_A ⟷ N ⟷ I

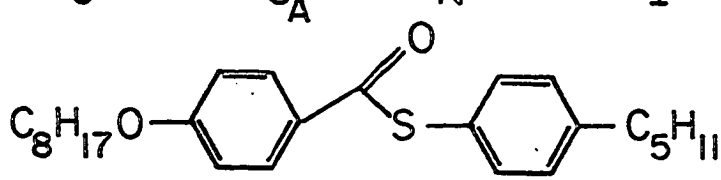

C ⟷ S_A ⟷ N ⟷ I

S_B ⟷ S_C

4-n-pentylphenylthiol-4-n-octyloxybenzoate (8S5)

positional order within the layers in either of these phases. In smectic A the molecules are aligned perpendicular to the layers so that there is one dimensional positional order. The system is optically uniaxial and the molecules are rotationally symmetric about the long axis. The smectic C phase, however, is optically biaxial because of a tilt angle between the normal to the layers and the director.

The smectic B phase is an ordered smectic phase where there is positional ordering and each layer forms a two dimensional solid. Molecules form a lattice within each layer but there is no long range correlation between layers.

The isotropic liquid phase occurs at a higher temperature than the smectic and nematic phases. As in any liquid there is no long range orientational or positional order. Schematic pictures of these liquid crystalline phases are shown in Figure 2.

Liquid crystals, with their myriad of phase transitions, offer an opportunity to study phase transition phenomena at accessible temperatures. In particular, the nematic-smectic A phase transition may exhibit a tricritical point or crossovers between different types of critical behavior.[1] Liquid crystals can also be useful for studying the effect of impurities on critical behavior.

Recently there has been extensive work done on the nematic-smectic A transition in the effort to determine if it can be a continuous (second order) transition and if so which class of critical behavior it exhibits. Several experiments are being done to measure the exponents ν and α whose values provide keys for understanding the microscopic behavior of the liquid crystalline phases, as well as interesting aspects of the phase diagram.

Figure 2. Schematics of several liquid crystalline phases. Smectics A and C are liquid-like smectics. B is more ordered with a lattice structure within each layer.

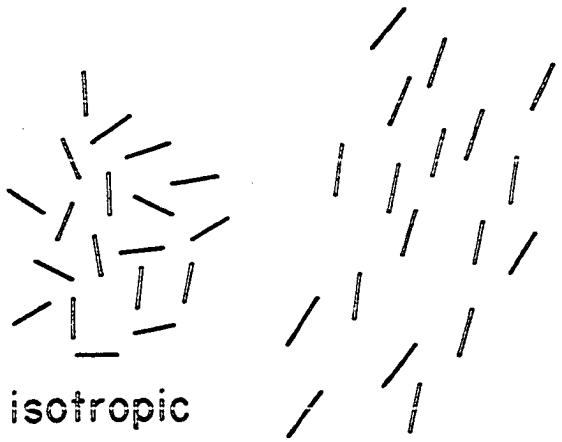

isotropic

nematic

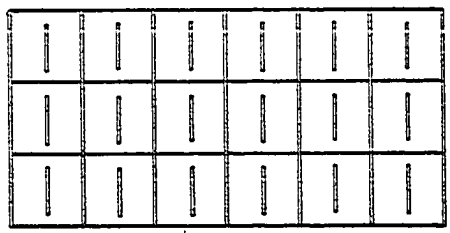

crystal

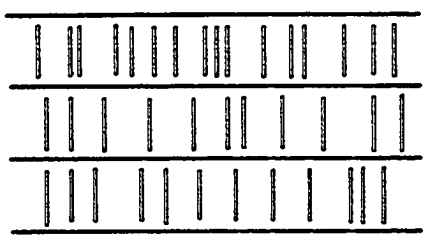

smectic A

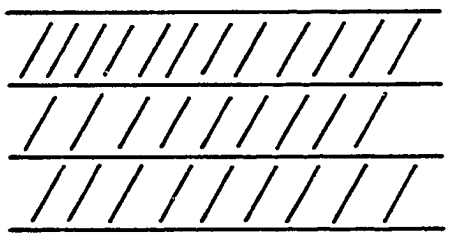

smectic C

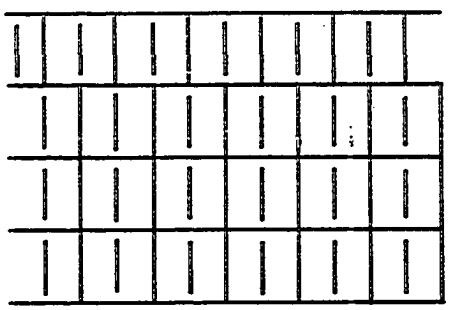

smectic B

The a.c. heat capacity method is a technique designed to measure small changes in heat capacity with resolution on the order of a part in 10^4 and temperature resolution of 1 mK. The high resolution in the measurement of temperature and heat capacity makes this an ideal method for determining the values of a critical exponent.

This thesis reports careful measurements of heat capacity near the nematic-smectic A transition in several liquid crystal compounds and the results for the exponent and other parameters in the equation for heat capacity at a critical point. Chapter 2 reviews previous theoretical and experimental work done on the nematic-smectic A transition. Chapter 3 describes the experimental techniques and the data fitting procedures. Chapter 4 presents the results for various compounds, including chemical analyses, and concludes the thesis with a discussion of the implications of these results on the understanding of the nematic-smectic A transition.

CHAPTER 2

THE NEMATIC-SMECTIC A TRANSITION: THEORY AND EXPERIMENT

2.1 The Order Parameters

The liquid crystalline phases are described by order parameters which can range from 0 to 1 depending on how ordered the system is. In the nematic phase

$$s = \tfrac{1}{2} \langle 3 \cos^2 \theta - 1 \rangle \qquad (2.1)$$

where θ is the angle between the long axis of each molecule and the director and s, the order parameter, is the average of the thermal fluctuations of the molecules around the director. S varies as a function of temperature and is typically in the range .3 to .8.[2/] In the smectic A phase the order parameter Ψ, a complex wave function, is a mass density wave

$$\Psi = \Psi_o \exp(iqz) \qquad (2.2)$$

where $|\Psi|^2$ is the strength of the smectic layering and $q=2\pi/d$ where d is the interlayer spacing. Although $\langle\Psi\rangle = 0$ in the nematic phase, both s and Ψ are needed to describe the smectic phase and there is coupling between them. As the smectic layers form it is energetically favorable for the long axes of the molecules to line up perpendicular to the layers. S, then, is high with a value of .8 or .9.[2/]

2.2 Microscopic Mean Field Theory

McMillan[3] and Kobayashi[4] have developed molecular mean field theories based on these order parameters and have produced a qualitatively correct phase diagram, shown in Fig. 3, for systems with nematic, smectic A, and isotropic phases. In a given homologous series, where the chemistry of the compounds differs by the length of their alkly chains, the temperature range of the nematic phase decreases as the alkyl chain increases and at some value of the chain length there is a tricritical point where the transition changes from second to first order. As the molecular length increases beyond the tricritical point the discontinuities in entropy and the order parameters increase. The variable, molecular length, is equivalent to the ratio of the nematic-smectic A transition temperature, Tna, to the nematic-isotropic transition temperature, Tni. Compounds which exhibit the nematic phase over a wide range in temperature, corresponding to a smaller Tna/Tni ratio, have maximized the orientational order before Tna is reached. There is no discontinuity in either order parameter at Tna and the transition is second order. Compounds with narrow nematic regions, or higher Tna/Tni ratio, do not have their orientational order saturated as they approach Tna. There is a discontinuity in the orientational order parameter s at Tna as it is energetically favorable for the molecules to line up perpendicular to the smectic layers as they form. The coupling of the order parameters s and Ψ forces a discontinuity in Ψ. Such discontinuities are characteristic of first order phase transitions, and are observable in compounds whose Tna/Tni ratio is greater than Tna/Tni at the tricritical point. Figure 4 shows plots of the order parameters as functions of temperature for first and second order transitions.

Figure 3. The phase diagram from the mean field theories of McMillan[3] and Kobayashi.[4] The nematic-smectic A transition temperature, Tna, increases with the length of the alkyl tail chain. At a critical value of chain length there is a non-zero entropy change at Tna and a first order phase transition.

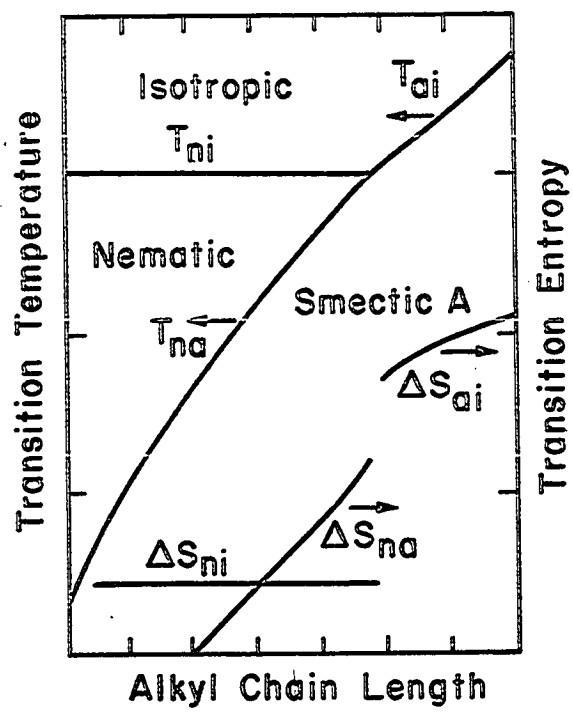

Figure 4. Discontinuities in the coupled order parameters s and Ψ as functions of temperature indicate a first order phase transition. A continuous variation in s and Ψ at Tna indicates a second order phase transition.

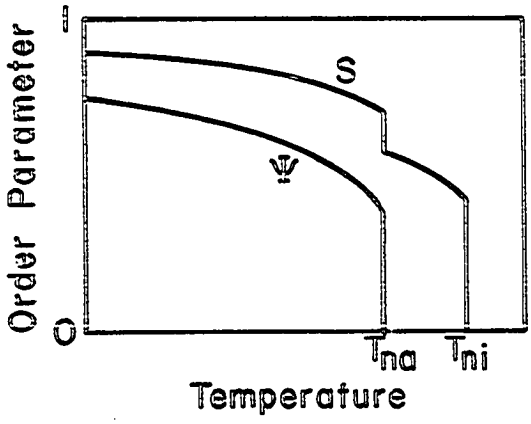

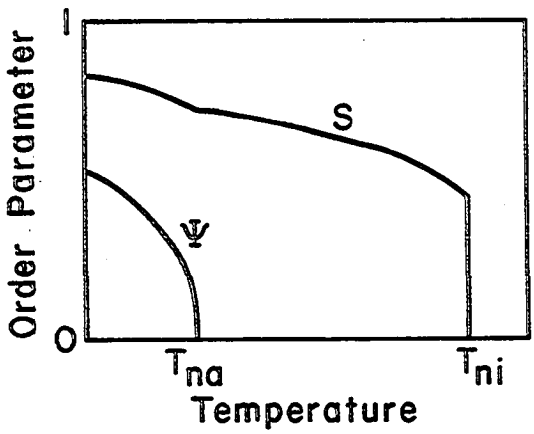

The mean field theories of McMillan[3] and Kobayashi[4] are the first to predict the existence of a tricritical point on the phase diagram and the possibility of a second order phase transition. There has been much experimental work aimed at locating the value of Tna/Tni for the tricritical point and at determining if there are second order nematic to smectic A phase transitions. Alben[5] has suggested that the search for the tricritical point could be carried out by doping a liquid crystal which has a second order nematic-smectic A transition with different amounts of a higher homolog which undergoes a first order transition, leading to a continuous variation of effective Tna/Tni with concentration. The proposed phase diagram for such a series of mixtures is illustrated in Figure 5 and resembles that of He^3-He^4 mixtures. That portion of the phase diagram where the concentration of the longer homolog is greater than the concentration at the tricritical point includes a coexistence region between the nematic and smectic A phases. Various groups doing measurements of latent heats on such mixtures have found the tricritical point in the range Tna/Tni = .85 to .96.[6] Many experiments have also been done to determine the order of the NA transition in pure CBOOA, which is believed to be near the tricritical point with a value of .94 for Tna/Tni. McMillan[7] does not observe a latent heat in the NA transition of CBOOA and Cabane and Clark,[8] in measuring s as a function of temperature using nuclear quadrupole resonance, do not observe a discontinuity in the order parameter. Both of these measurements indicate a second order NA transition. Contradicting these results, Torza and Cladis[9] measure a slight volume discontinuity and Djurek *et al.*[10] measure small latent heats at Tc indicating a first order transition. These varying results for CBOOA

Figure 5. A proposed phase diagram for mixtures of liquid crystals resembling the phase diagram for He^3-He^4 mixtures. x_I is the concentration of the liquid crystal with a longer end chain. The average length of the end chain increases with greater concentrations of the longer homolog. At a certain average length the tricritical point is reached and there is a coexistence region between the nematic and smectic A phases, indicating a first order transition.

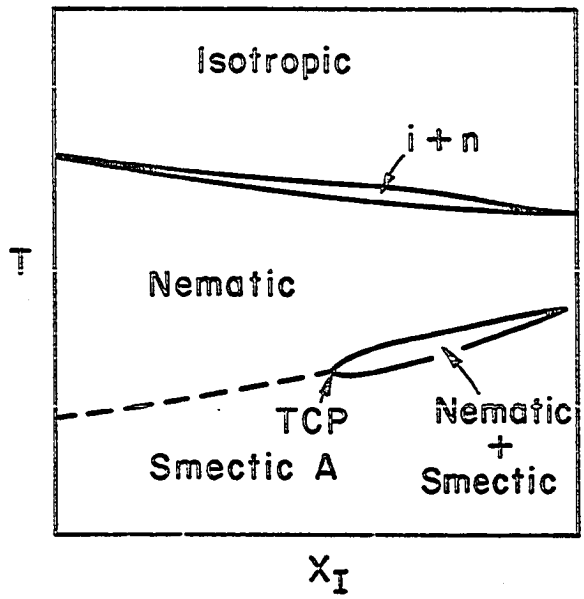

may be explained by the nearby presence of the tricritical point where chemical differences such as small concentrations of shorter molecules, either homologs or broken segments of CBOOA, can determine whether the sample exhibits first or second order behavior. The effects of chemical impurities on liquid crystal phase transition physics are discussed in detail in Chapter 4.

2.3 The Landau Free Energy and Analogy with a Superconductor

DeGennes[11] and McMillan[12] have proposed a Landau theory where the free energy incorporates the coupling of the smectic order parameter to the nematic director.

$$F_1 = \int d\vec{r}\left[A(T)\ |\Psi|^2 + \frac{B}{2}\ |\Psi|^4 + C_{||}\ |(\vec{n}\cdot\vec{\nabla}-iq)\Psi|^2 + C_{\perp}|\vec{n}\times\vec{\nabla}\Psi|^2\right] . \quad (2.3)$$

The $C_{||}$ term expresses the cost in energy of compressing the smectic layers and the $C_{\perp}$ term represents the cost of rotating the director within the layers. Only even powers appear in the free energy as it must be invariant under changes in the phase of Ψ. The coefficient A is positive in the nematic phase and goes to zero at Tna. The sign of the coefficient B determines the order of the phase transition.

$$B = B_o - 1/2C^2\chi \quad (2.4)$$

where C is a constant combining $C_{||}$ and $C_{\perp}$ from the coupling terms, B_o is positive, and χ is a response function which is large and positive when there are large fluctuations in the order parameter s. If the order parameter s is saturated near Tna, as in the case of a wide nematic phase, χ is small so B is positive, and the transition is second order. If χ is large enough to make B negative, as in compounds with a narrow nematic

region, then a Ψ^6 term must be added to ensure stability and the resulting plots of $F(\Psi)$ show that at Tna F is minimized at a non-zero Ψ, and the transition actually occurs at a higher temperature, Tc > Tna, and is first order.

DeGennes[13] has noted that this expression resembles the Ginsberg-Landau free energy of a superconductor where the coupling between the director and smectic order parameter is analagous to the coupling of the magnetic vector potential with the order parameter. The order parameter in both the superconductor and liquid crystal has two components, the amplitude and phase. In the superconductor the zero temperature coherence length is hundreds to thousands of angstroms long causing mean field like behavior. In a liquid crystal, where the interactions are short ranged and the coherence length is on the order of a molecular length, helium-like behavior is expected. Based on this analogy DeGennes[11] predicts the helium values, $\nu=.66$ and $\alpha=0$, for the critical exponents near the nematic-smectic A phase transition. DeGennes has also predicted that the smectic A phase excludes the bend and twist distortions described below, as a superconductor excludes magnetic flux.

In Figure 6 the twist, bend, and splay distortions are illustrated. The bend and twist modes are excluded in the smectic phase as such distortions break up the interlayer spacing and cost energy. A splay distortion maintains the interlayer spacing and does not cost as much energy. The following terms which describe these fluctuations of the director are included in the free energy,

$$F_2 = \int d\vec{r}\left[\frac{1}{2} K_{11}(\vec{\nabla}\cdot\vec{n})^2 + \frac{1}{2} K_{22}\left[\vec{n}\cdot(\vec{\nabla}\times\vec{n})\right]^2 + \frac{1}{2} K_{33}\left[\vec{n}\times(\vec{\nabla}\times\vec{n})\right]^2 - \chi_a(\vec{n}\cdot\vec{H})^2\right], \tag{2.5}$$

Figure 6. A schematic illustration of the splay, bend, and twist fluctuations.

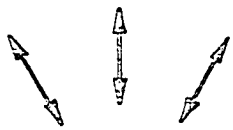

Splay (div $\vec{n} \neq 0$)

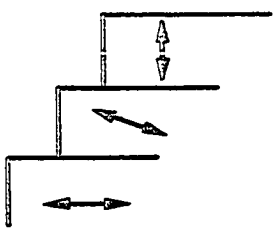

Bend (curl $\vec{n} \perp \vec{n}$)

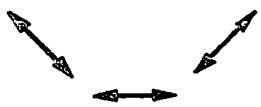

Twist (curl $\vec{n} \parallel \vec{n}$)

where $F_{total} = F_1 + F_2$. The Kii are the elastic constants (splay, twist, and bend) and the last term lowers the free energy when the molecules are aligned in a magnetic field.

2.4 Critical Exponents

The thermal average of $\langle\Psi\rangle$ is positive in the smectic phase, decreases as temperature approaches Tc, (Tc = Tna for a second order phase transition), and drops to zero in the nematic phase. Although $\langle\Psi\rangle$ vanishes in the nematic phase there are fluctuation effects whereby short range order persists over a distance $\xi(T)$ larger than the molecular length. Droplets with smectic A ordering whose dimensions are the components of the correlation length, $\xi(T)$, parallel and perpendicular to the director, form in the nematic phase and increase in size as Tc is approached from above.

$$\xi_{\perp} \propto \left[(T-Tc)/Tc\right]^{-\nu_{\perp}} \tag{2.6}$$

$$\xi_{||} \propto \left[(T-Tc)/Tc\right]^{-\nu_{||}} \tag{2.7}$$

where $\nu_{\perp}$ and $\nu_{||}$ are non-integral exponents. As the smectic fluctuations are enhanced it costs more energy to bend or twist the director. This is expressed in the renormalization of the elastic constants which grow as functions of $\xi_{||}$ and $\xi_{\perp}$.

The growth of the smectic fluctuations results in the increase of other physical quantities near Tc as functions of reduced temperature, t, raised to a non-integral exponent, where t = (T-Tc)/Tc. The heat capacity near a critical point is proportional to $t^{-\alpha}$ where α is a critical exponent and is the same on both sides of the transition. There exist several

classes of phase transitions characterized by the values of the critical exponents. A correct determination of critical exponents near the nematic-smectic A transition could place this transition in a universality class and provide better understanding of the physics near Tc using our knowledge of other systems in that class.

There are only a few groups measuring critical exponents on the nematic-smectic A transition and the results of their experiments vary considerably. Johnson et al., in an a.c. heat capacity experiment, have measured α in pentylphenylthiol-octyloxybenzoate ($\overline{8}S5$)[14] and in octyloxy-cyanobiphenyl (8OCB)[15] and find alpha near zero indicating the logarithmic behavior of a superfluid-like transition. In their 8OCB measurements they observe a 40 mK flattened region at the transition. This could be a two phase region which is characteristic of a first order phase transition. In another a.c. heat capacity experiment Garland[16] has measured alpha between .2 and .3 on 8OCB and also on octylcyanobiphenyl (8CB). Birgeneau[17,18] at MIT has used light scattering and high resolution x-ray scattering to obtain values for $\nu_{||}$ and $\nu_{\perp}$ for 8OCB, 8CB, and CBOOA (cyanobenzyloxyoctylaniline). Using the anisotropic version of the Josephson scaling law,[19]

$$2\nu_{\perp} + \nu_{||} = 2-\alpha \quad , \tag{2.8}$$

the exponents $\nu_{\perp}$, $\nu_{||}$, and α are related to one another. In Table 1, Birgeneau's results on the various compounds are shown as well as the values for alpha obtained from the Josephson scaling law by inserting his measured values of $\nu_{||}$ and $\nu_{\perp}$. 8OCB is the one compound that has been measured by all three of these groups resulting in values for α of 0 (Johnson),[15] .25 (Garland),[16] and .13 (Birgeneau).[17,18] This thesis reports the results

of our high resolution a.c. heat capacity measurements on 8OCB, 8CB, CBOOA, $\overline{8}S5$, and CBNOA and attempts to clarify the confusion surrounding the nematic-smectic A transition.

TABLE 1

X-RAY RESULTS FOR $\nu_{||}$ AND $\nu_{\perp}$ AND CALCULATED α

Compound	$\nu_{\|\|}$	$\nu_{\perp}$	α
CBOOA	.70±.04	.62±.05	.06±.14
8OCB	.71±.04	.58±.04	.13±.12
8CB	.67±.04	.51±.04	.31±.12

CHAPTER 3

HEAT CAPACITY EXPERIMENTS

3.1 The A.C. Method

The a.c. calorimeter used for the measurements is a modification of the one originally designed by J. E. Smaardyk,[20,21] and is based on the a.c. heat capacity technique of Sullivan and Seidel.[22] An oscillating voltage is applied across a thin film heater in contact with the sample. The resulting temperature oscillations, which are inversely proportional to heat capacity, are measured as a function of temperature by a thin film thermocouple underneath the sample.

A schematic model of an a.c. calorimeter is shown in Figure 7. The heat flow from the thin film heater on the sample, meaning the heater-liquid crystal assembly, to the heat sink has radial and perpendicular components. By adding exchange gas behind the window as a thermal link between the sample cell and heat sink, the perpendicular thermal conductivity becomes much greater than the radial thermal conductivity. The change in the energy of the sample complex can be written as follows:

$$C\frac{dT}{dt} = \frac{V^2(t)}{R} - K_{\perp}(T-T_o) \quad , \qquad (3.1)$$

where C is the heat capacity of the sample, $K_{\perp}$ is the thermal conductance from the sample cell through the exchange gas underneath, R is heater resistance, and T_o is the temperature of the heat sink or thermal bath. If

Figure 7. Schematic model of a.c. calorimetric technique. Kinternal is the thermal conductivity through the sample complex from the thin film heater to the thermocouple. $K_{\perp}$ is the perpendicular component of thermal conductivity from the thermocouple through the gas to the bath. The exchange gas ensures that the perpendicular components of thermal conductivity are much greater than the parallel components. The heat capacity measured, C, is the heat capacity of the entire sample assembly.

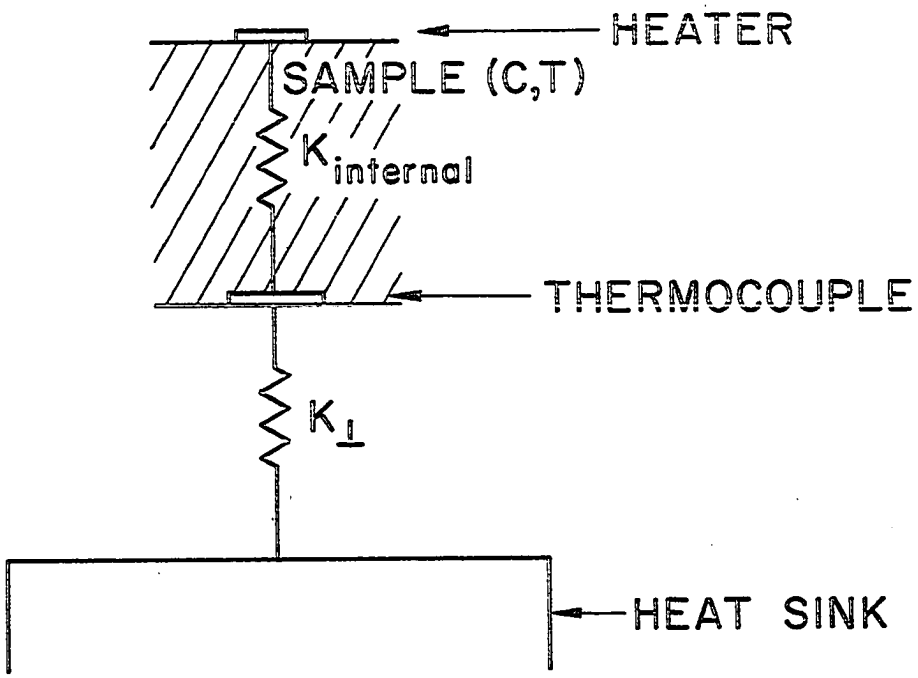

V(t) is a sinusoidal voltage of amplitude V_o and frequency $\omega/2$, the equation can be solved for T where

$$T = T_o + V_o^2/2R \left[1/K_{\perp} + 1/\omega C \frac{\sin(\omega t+\phi)}{\left(1+1/\omega^2\tau^2_{ext}\right)} \right]$$

$$= T_o + Tdc + Tac \sin(\omega t+\phi) \quad . \tag{3.2}$$

$\tau_{ext} = C/K_{\perp}$ is the thermal relaxation time of the sample to the bath and $\phi = \prod + \tan 1/\omega\tau_{ext}$. The dc temperature rise of the sample,

$$Tdc = V_o^2/2RK_{\perp} \quad , \tag{3.3}$$

is the averaged difference between the sample temperature and the heat sink temperature where $V_o^2/2R$ is the average power. If $\omega\tau_{ext} >> 1$ then Tac, the amplitude of the a.c. component of temperature, simplifies to:

$$Tac = V_o^2/2R\omega C \quad , \tag{3.4}$$

and the heat capacity C can be calculated from the amplitude of the temperature oscillation. This condition defines a lower limit on the frequency range for the a.c. technique.

The upper limit of this range is defined by the internal relaxation time:

$$\tau in << 1/\omega \quad , \tag{3.5}$$

in other words, the sample must not have internal temperature gradients. $\tau in = C/Kin$ where Kin is the thermal conductance from the thin film heater on top of the sample cell to the thin film thermocouple on the glass. The

thermal wavelength associated with the internal relaxation time,

$$\ell = \sqrt{k_{in}/\omega c} \quad , \tag{3.6}$$

where k_{in} is thermal conductivity and c is heat capacity per unit volume of the sample complex, is the length which determines how thick the sample cell can be so that all parts of it oscillate in phase.

Before each measurement a frequency response curve is plotted to find the range of frequency where heat capacity is not a function of frequency. C is inversely proportional to $\omega\tau_{ac}$ so by plotting $\omega\tau_{ac}$ against ω, a flat frequency response is obtained whose limits are determined by the reciprocals of the internal and external relaxation times described above. The a.c. calorimeter must be operated in this frequency range. An example of such a frequency response curve is shown in Figure 8.

3.2 The Liquid Crystal Sample Cell

A schematic of the liquid crystal sample cell is shown in Figure 9. A pyrex window, several microns thick, is epoxied onto a copper mount with Stycast 1266.[23] The copper mount is 3 cm. in diameter and in its center is a hole with a diameter of 0.5 cm. It is important for the support of the glass that the epoxy reach the edge of the hole. The amplitude of the temperature oscillation is measured with a thin film copper-bismuth thermocouple. A 7K Å thick film of bismuth is evaporated from a tungsten strip onto the glass and then, while still under vacuum, the copper mount covered by the pyrex window is rotated 90° over the mask and a 2.5K Å film of copper is deposited across the bismuth from a tungsten strip. This method ensures that no oxides form between the metal layers. The configuration of the thermocouple junctions on the glass is depicted in Figure 10.

Figure 8. The flat region of the frequency response curve determines the operating range for the a.c. technique. Heat capacity is inversely proportional to fxTac. The operating range is determined by the reciprocal of the internal relaxation time $1/\tau_{int}$ and the reciprocal of the external relaxation time $1/\tau_{ext}$.

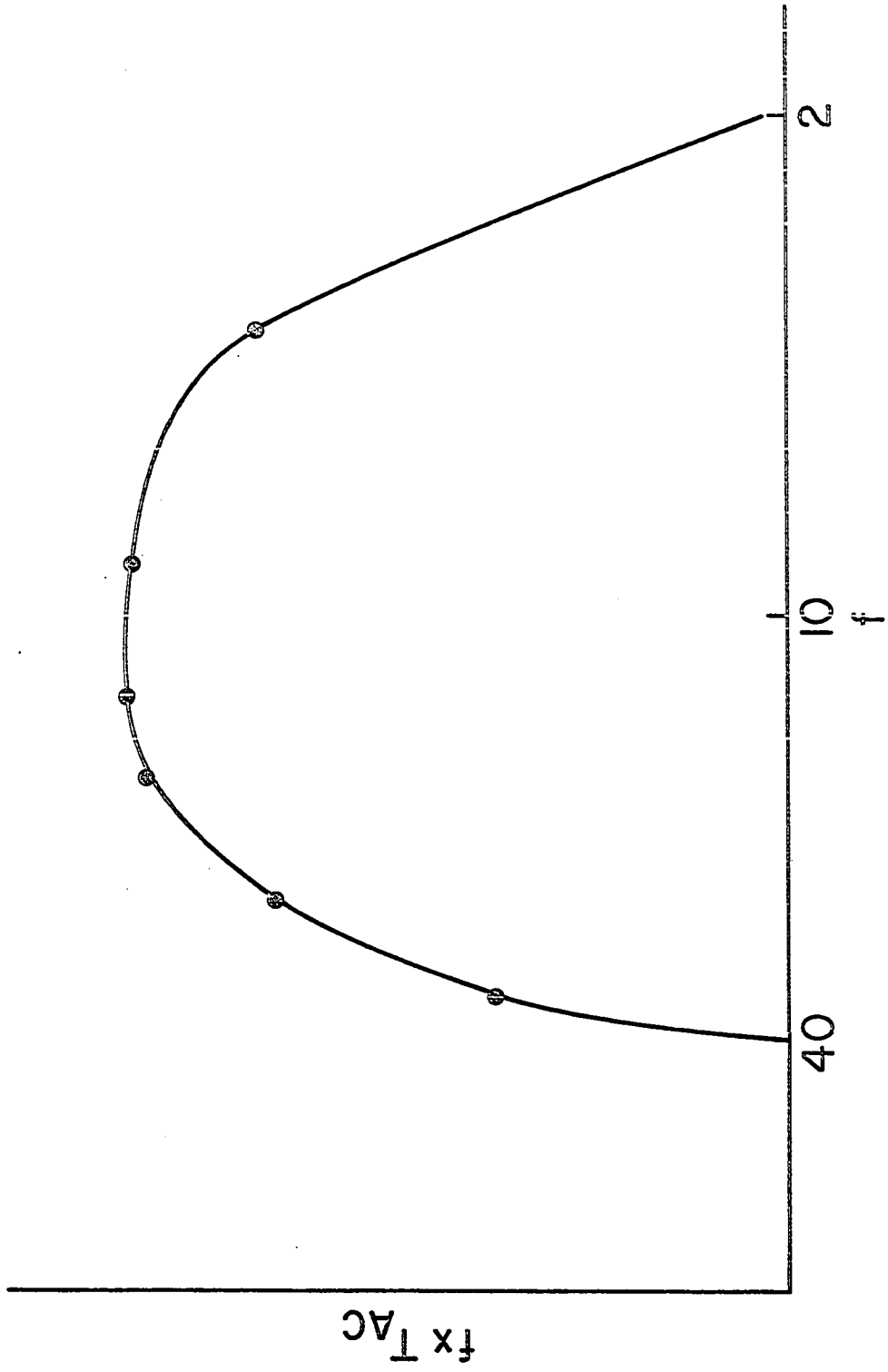

Figure 9. The experimental cell for the a.c. heat capacity measurements of liquid crystal. A pyrex window with a thin film thermocouple junction in its center is epoxied over a hole in a copper disk. The liquid crystal lies between the pyrex window and a sheet of mylar with a thin film heater on its top. Several torr of exchange gas behind the window ensures perpendicular heat flow from the thin film heater.

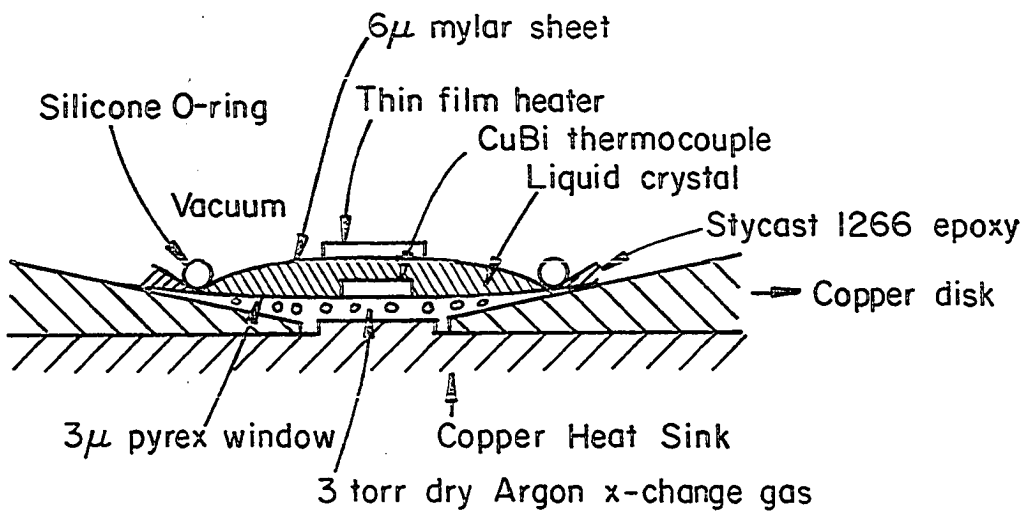

Figure 10. Configuration of bismuth-copper thermocouple used to measure temperature oscillations of liquid crystal.

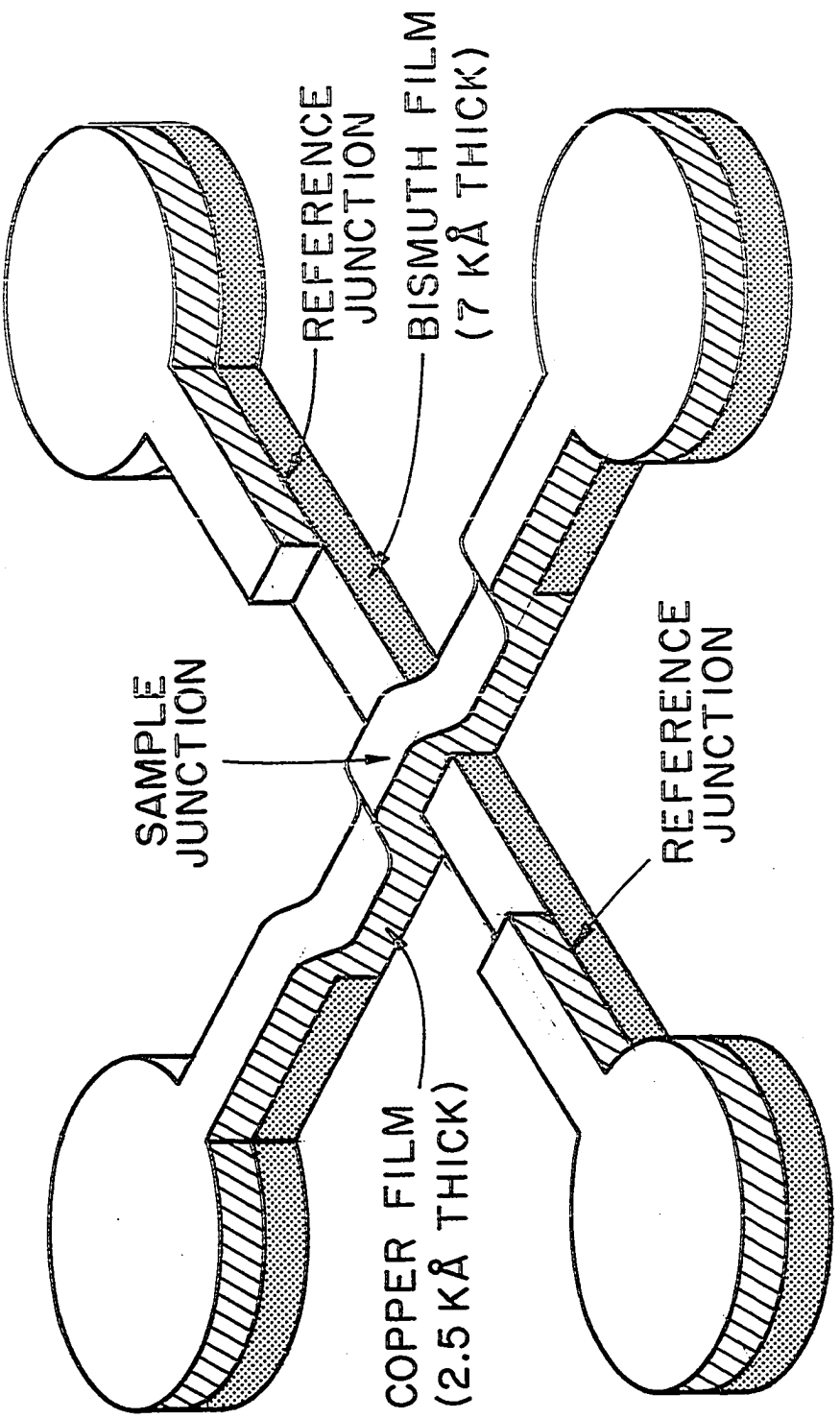

The resistance between the junctions is about 10 Ω and the thermoelectric power is on the order of 50 μv/°K. Attached to the glass is a 6 μ thick, 1.27 cm diameter mylar[24] disk on which are evaporated the heater and its leads. The heater is a 2 mm × 2 mm square of Chromel A,[25] 100 Å thick, and the leads are thin silver films on the order of 500 Å thick. These films are evaporated from tungsten strips in the configuration shown in Figure 11 during the same vacuum cycle to prevent oxidation between the metals. This is done by supporting the mylar disk over a wheel containing the masks, which is rotated between evaporations to bring the proper mask into position. The Chromel A film extends under the silver leads for better adhesion between the films. The heater resistance ranges from 100-500 Ω depending on the actual thickness of the Chromel A film. The thicknesses of all the metal films are monitored by a Kronos film thickness moniter attached to a quartz crystal oscillator inside the evaporator.

The mylar is attached to the glass with the heater film on top using a drop of Torr Seal[26] between the heater leads. The copper mount with the mylar on it is placed underneath a weight while the Torr Seal is applied. It is important that the thermocouple junction be directly underneath the heater so that there will be no temperature gradient across it. Silver wires, .002" in diameter and 99.99% pure, are attached to the edges of the silver films under microscope with small dabs of silver epoxy[27] on the silver films and on the glass. 10 mil silver wires (99.95% pure) are then attached to the tabs of the thermocouple junctions and to the end of the 2 mil silver wires from the heater films using more silver epoxy. The silver epoxy provides electrical contact with lower contact resistance when used with silver wire. These silver wires are further supported by

Figure 11. Configuration of thin film heater. Heater is a 2 mm × 2 mm square of Chromel A, 100 Å thick, and the leads are 500 Å thin silver films.

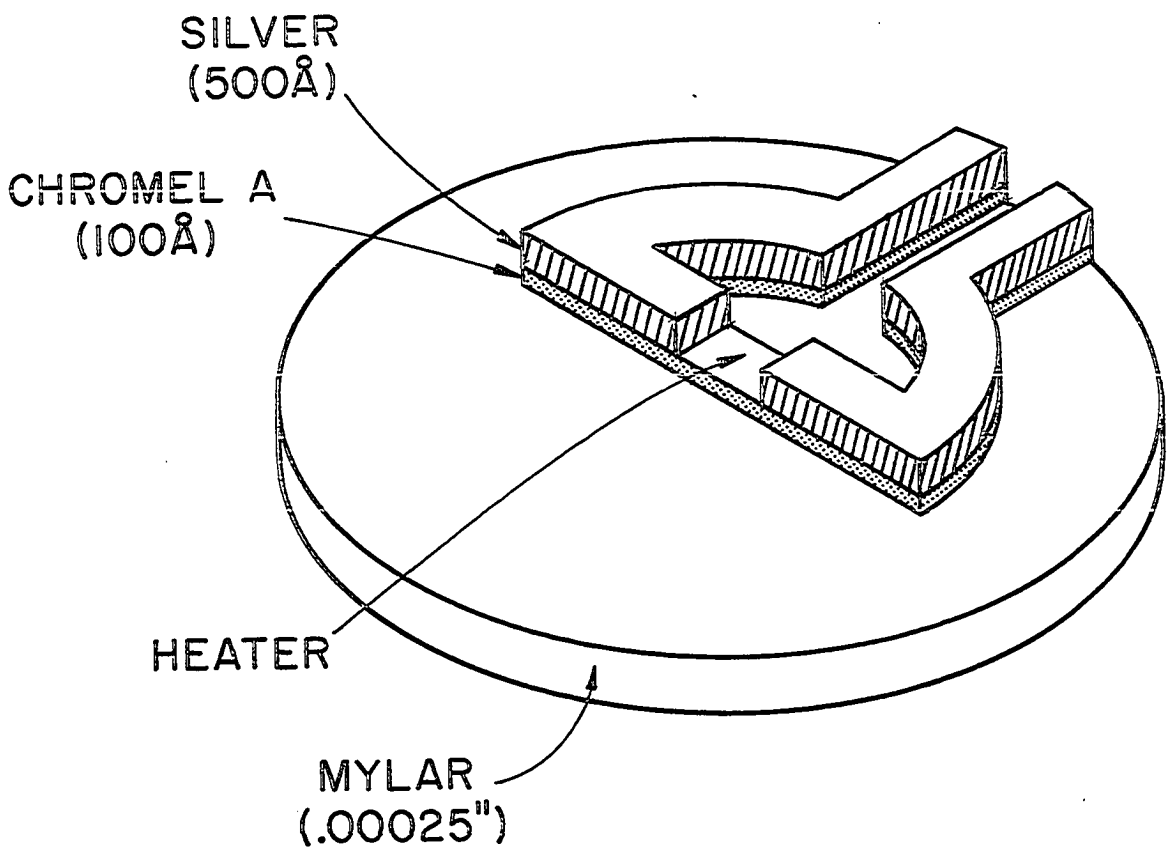

dabs of Torr Seal holding them on the outer edge of the pyrex window. A top view of the completed sample mount is shown in Figure 12.

The sample mount is bolted onto a heat sink (the thermal bath), which sits on three stainless steel pins in a vacuum can. There are two leads from the reference and center junctions and each pair is twisted in parallel to minimize the noise. The reference junction is grounded using silver epoxy. The silver leads are soldered to #32 copper wires going to the outside of the vacuum can. A copper button, which is slightly smaller than the hole in the copper mount protrudes from the heat sink, and is lined up directly underneath the thermocouple junction for better perpendicular thermal conductivity. After the vacuum can is pumped out several torr of dry argon gas are let in behind the window. A cross-sectional view of the assembled calorimeter is shown in Figure 13.

Sealing the liquid crystal between the mylar and glass is the most difficult aspect of the experiment. The measurements are of small changes in heat capacity, which are meaningful only if there are no small drifts in the amount of sample sealed. The clamping device, which is used to seal the sample cell, is illustrated in Figure 14. A silicone O-ring,[28] .01" in diameter, is dropped onto the mylar under vacuum and held in place by a screw pushing against the brass button holding the O-ring. In addition, several drops of Stycast 1266 are added around the edge of the mylar to ensure that no liquid crystal will seep out from underneath the O-ring.

3.3 The Liquid Crystal Samples

The samples measured were all shown in Figure 1. The first experiments were done on octyloxycyanobiphenyl (8OCB),[29] which was chosen for

Figure 12. Top view of sample mount. Silver epoxy is used for mechanical and electrical contact between heater and thermocouple films and silver wires. Torr Seal is used to adhere the mylar disk to pyrex.

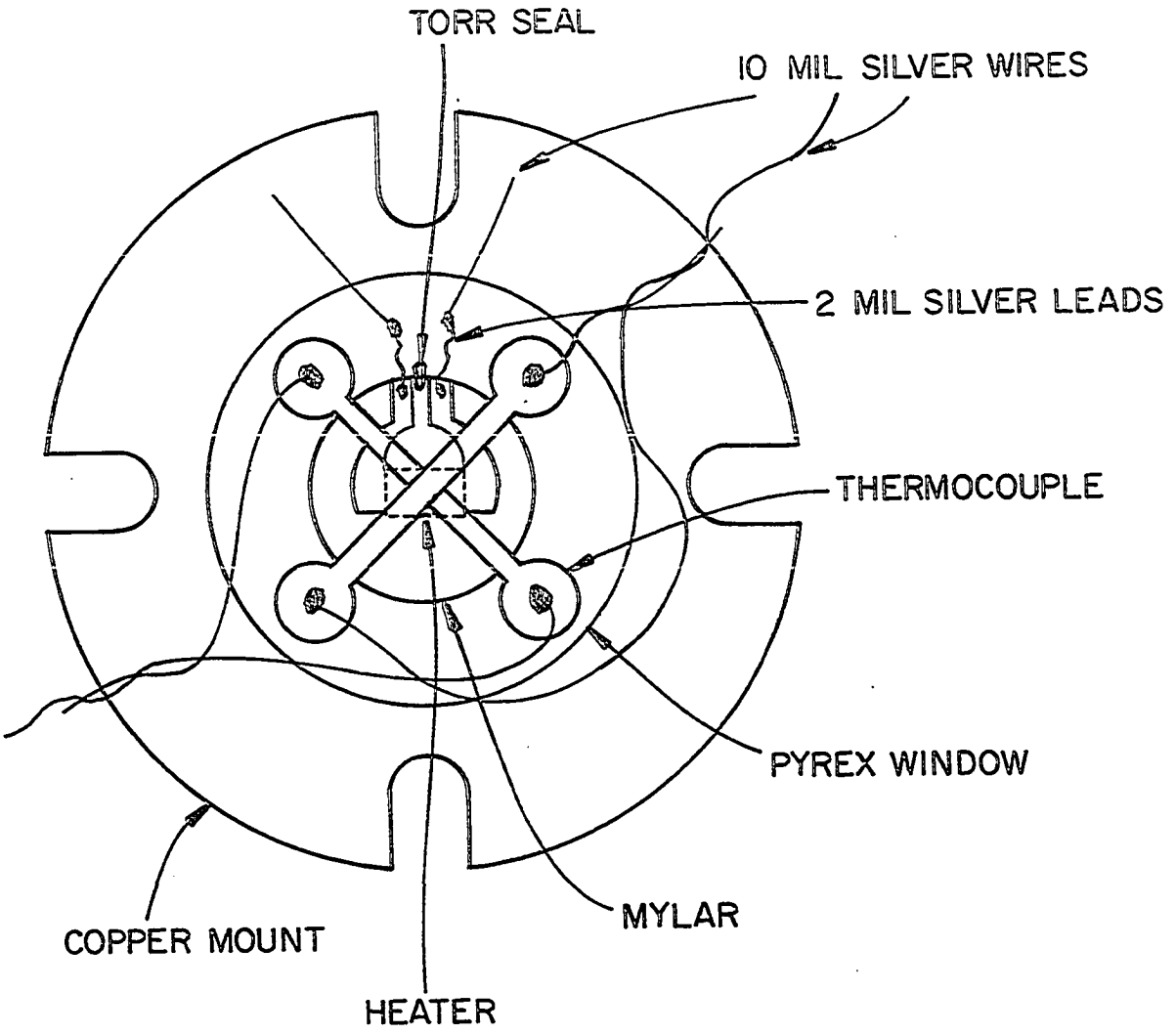

Figure 13. Cross-sectional view of assembled calorimeter. Copper sample mount is bolted onto copper heat sink. Protruding copper button and exchange gas behind window ensure better perpendicular thermal conductivity.

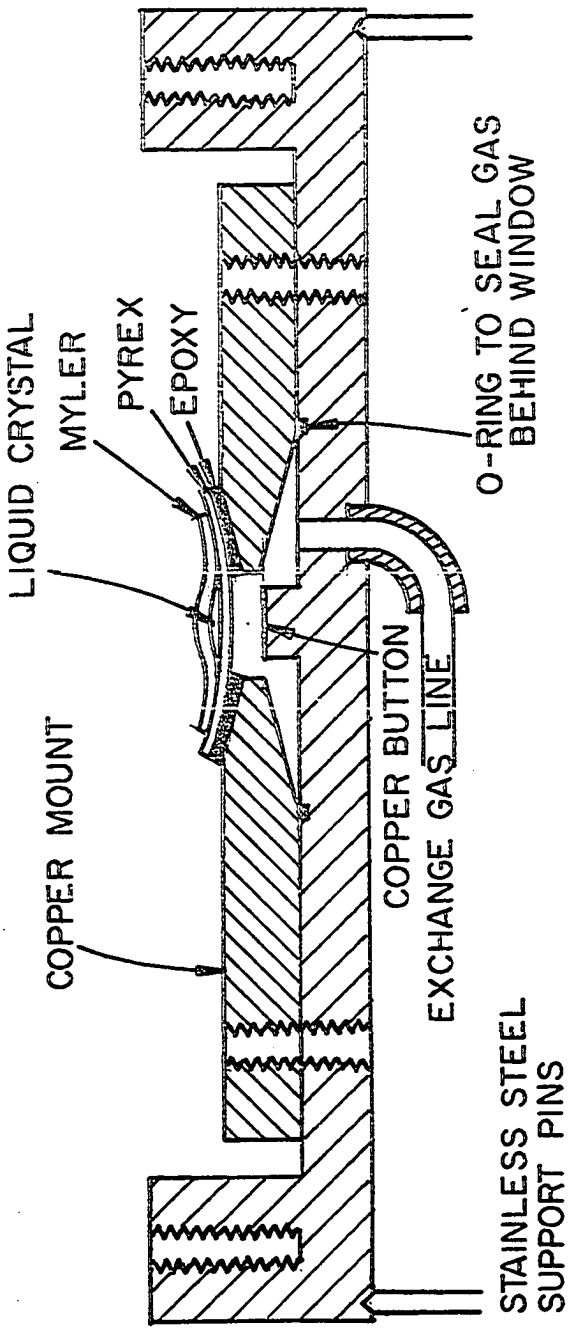

Figure 14. Illustration of clamping procedure to seal liquid crystal. O-ring on the brass piece is held onto the clamping bar with a brass clamp. The pointed screw is engaged from the outside and turned until the O-ring drops into place on the mylar.

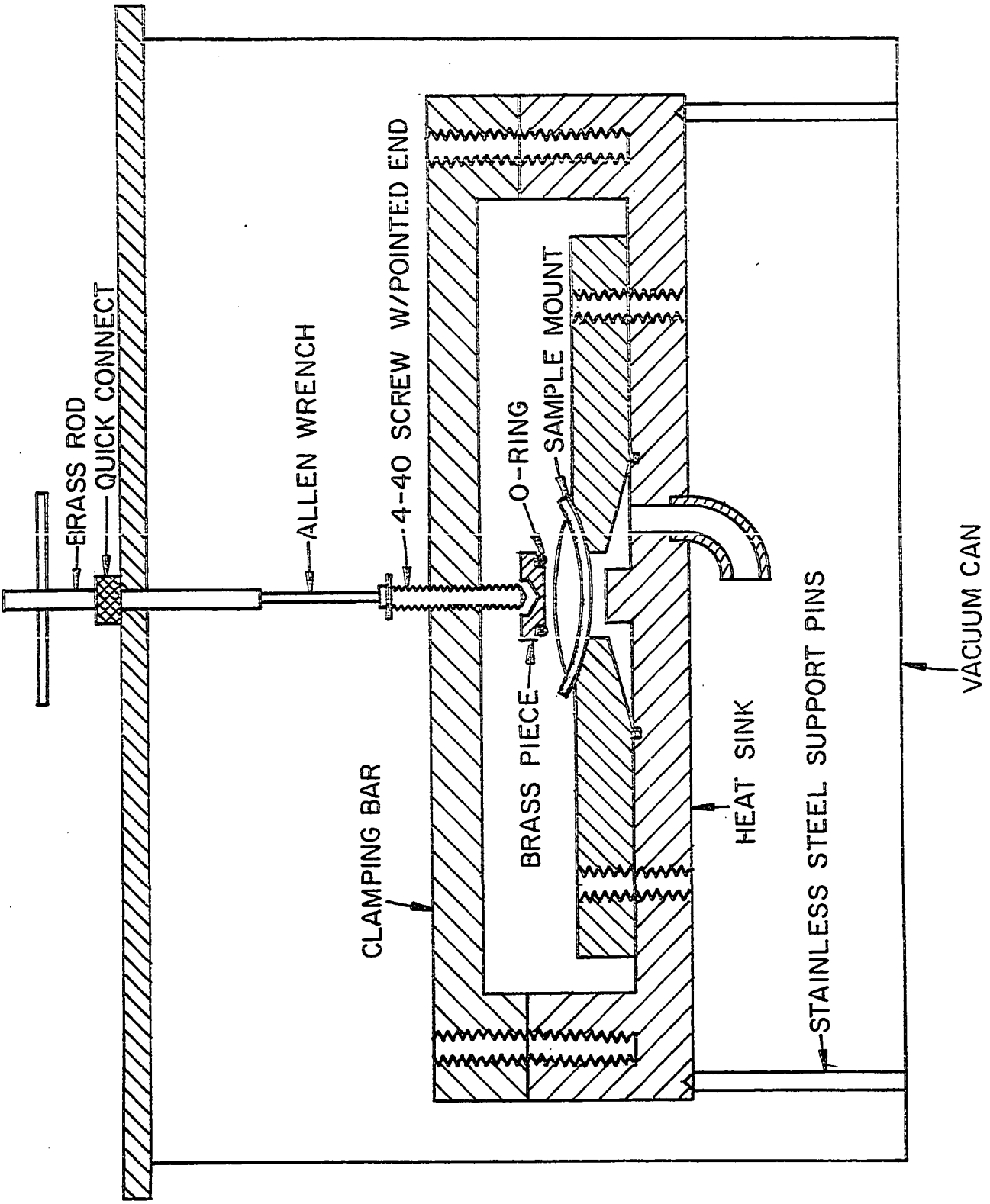

its chemical stability. The measurements were done on two different samples from different batches of 8OCB made by British Drug Houses.[30] The first sample came from the earliest batch made by BDH. It was sent to us by P. E. Cladis and had been further purified by vacuum sublimation. The second sample, given to us by D. L. Johnson, was from a later BDH batch and had not been further purified.

Octylcyanobiphenyl (8CB), also made by BDH, was sent to us by D. L. Johnson without further purification.

4-n-pentylbenzenethio-4'-n-octyloxybenzoate ($\overline{8}$S5) was sent to us by D. L. Johnson and had been recrystallized five times from ethanol by Mary Neubert and T. A. Santors.

Cyanobenzylidene-octyloxyaniline (CBOOA) was obtained from Eastman[31] (compound #11963). 500 mg of CBOOA were recrystallized from 1 ml benzene and 7 ml of hexane. The solution was refluxed, then cooled to recrystallize the CBOOA. The material was filtered and the above process repeated several times. The sample was melted and recrystallized to separate off the solvent.

Cyanobenzylidene-nonyloxyaniline (CBNOA), a higher homolog of CBOOA with a nine carbon tail, was synthesized by Smaardyk. Approximately 500 mg of this batch were recrystallized three times in ~20 ml of ethanol. The recrystallization procedure was the same as described for CBOOA.

All samples were stored in a dessicator and handled with clean tweezers. The calorimeter was baked out at 90° C for several hours before any sample was added. After being placed in the calorimeter each sample was heated under vacuum to a temperature above the melting point and was pumped on for about thirty minutes before it was sealed. This process should have driven off any volatile impurities. A cold trap filled

with liquid nitrogen protected the unsealed sample from oil vapors from the diffusion pump.

3.4 The Electronics and Measuring Techniques

A PET microcomputer[32] is used to control and measure the amplitude of the temperature oscillations. The root-mean-square amplitude of these oscillations is varied from 1 to 10 mK depending on the resolution desired. A block diagram of the electronics used to measure the temperature oscillations of the sample is shown in Figure 15. A Hewlett Packard Model 3300A function generator supplies the sinusoidal voltage for the thin film heater and the reference input for the lock-in measuring the temperature oscillations. This voltage is attenuated and passes through a voltage follower and a resistor in series with the heater, whose value is equal to the heater resistance. The rms average of the power across the heater ranges from 20 to 400 μ watts. The d.c. temperature rise of the sample above the heat sink is calculated by plotting the apparent transition temperature for the nematic-smectic A transition as a function of heater power and extrapolating to zero heater power. The a.c. temperature difference between the heat sink and sample corresponds to the a.c. voltage between the reference and center junctions of the thermocouple. For a rms temperature oscillation of 5 mK the voltage between the thermocouple junctions would be several tenths of a microvolt. This voltage is amplified through a P.A.R. AM1 transformer and P.A.R. 113 preamplifier and then measured with a P.A.R. 128 lock-in amplifier in the 2f mode. The total gain of the electronics is roughly a million. The output of the 128 is monitored by a DANA Model 5333 digital voltmeter which is interfaced to the PET microcomputer. A multiplexer permits use of the DVM in measuring several

Figure 15. A block diagram of the electronics of the a.c. calorimeter.

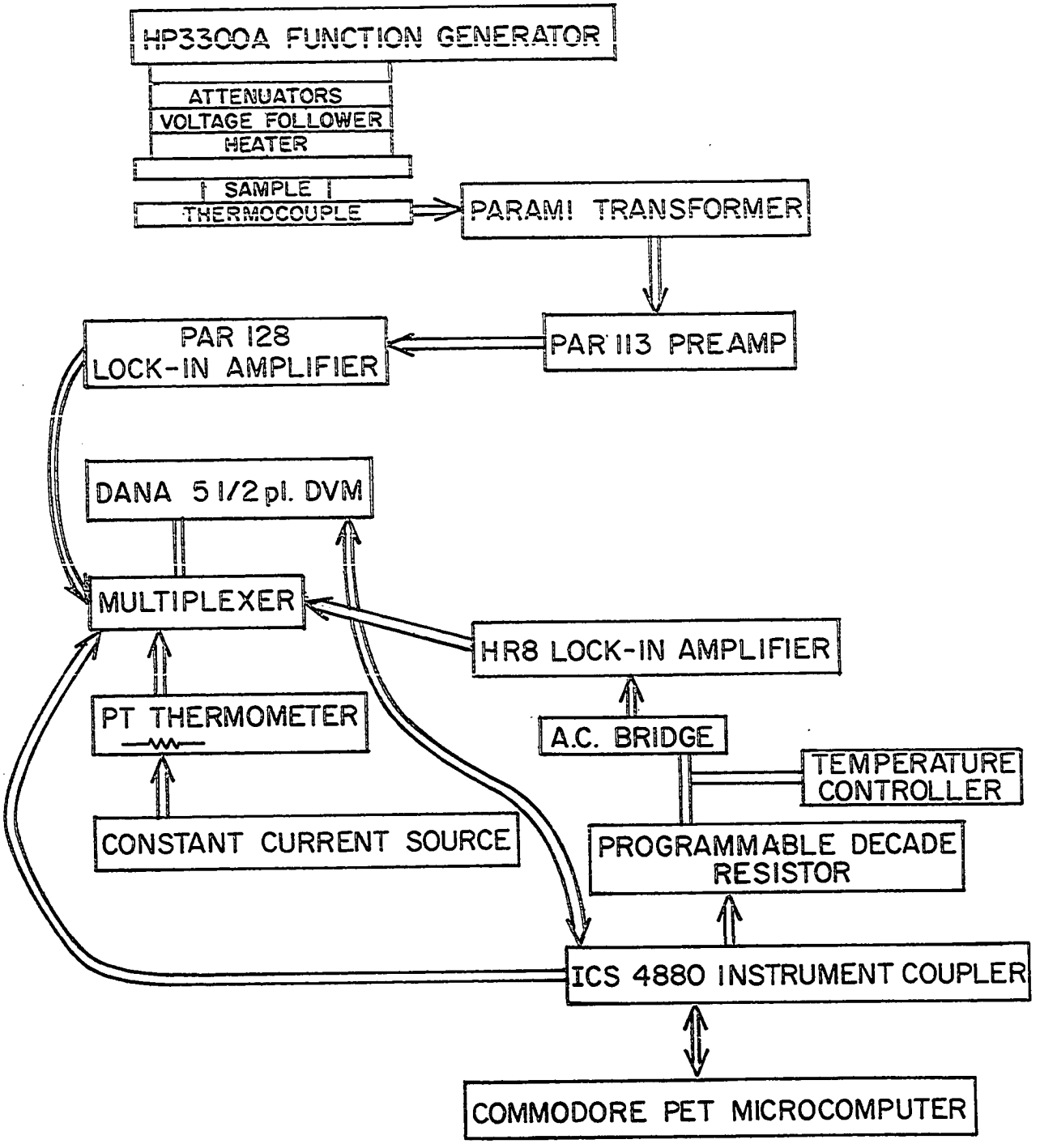

different voltages in the experiment. The interface between the PET and voltmeter is the ICS Electronics Corporation Model 4880 Instrument Coupler which can be connected between an IEEE 488 port and any digital instrument and can either transfer information to the PET from a measuring device or commands from the PET to the various devices. At each temperature 60-200 readings of the DVM output, taken at 1 second intervals, are averaged and that average and its standard deviation are recorded on tape by the PET.

The vacuum can and heat sink each have heater wires wound on them and are covered with Sauereisen cement.[33] The vacuum can's temperature is controlled by a d.c. bridge.[20] The temperature control circuit for the heat sink is shown in Figure 16, where one leg of the a.c. bridge is a General Radio Model 1435 Programmable Decade Resistor which is interfaced to the PET. The temperature of the heat sink is changed by taking discrete steps in resistance which correspond to temperature jumps of 1 to 20 mK. At each step the output of the a.c. bridge is monitored by a P.A.R. HR8 Lock-in amplifier connected to the DANA 5333 which is interfaced with the PET. The PET steps the resistance and then waits for the HR8 output to reach a null, $V \leq 1$ volt, before taking the experimental data. The temperature of the bath is measured with a platinum thermometer[34] hooked to a constant current source and to the DVM. Both before and after the averaging of the 128 signal the voltage across the platinum thermometer is measured with two directions of current, averaged, and recorded by the PET. In Figure 17 a flow chart of the BASIC program used to control the experiment and take the data shows the order of the various control steps and measurements for each data point.

Figure 16. The a.c. bridge used to control the temperature of the heat sink.

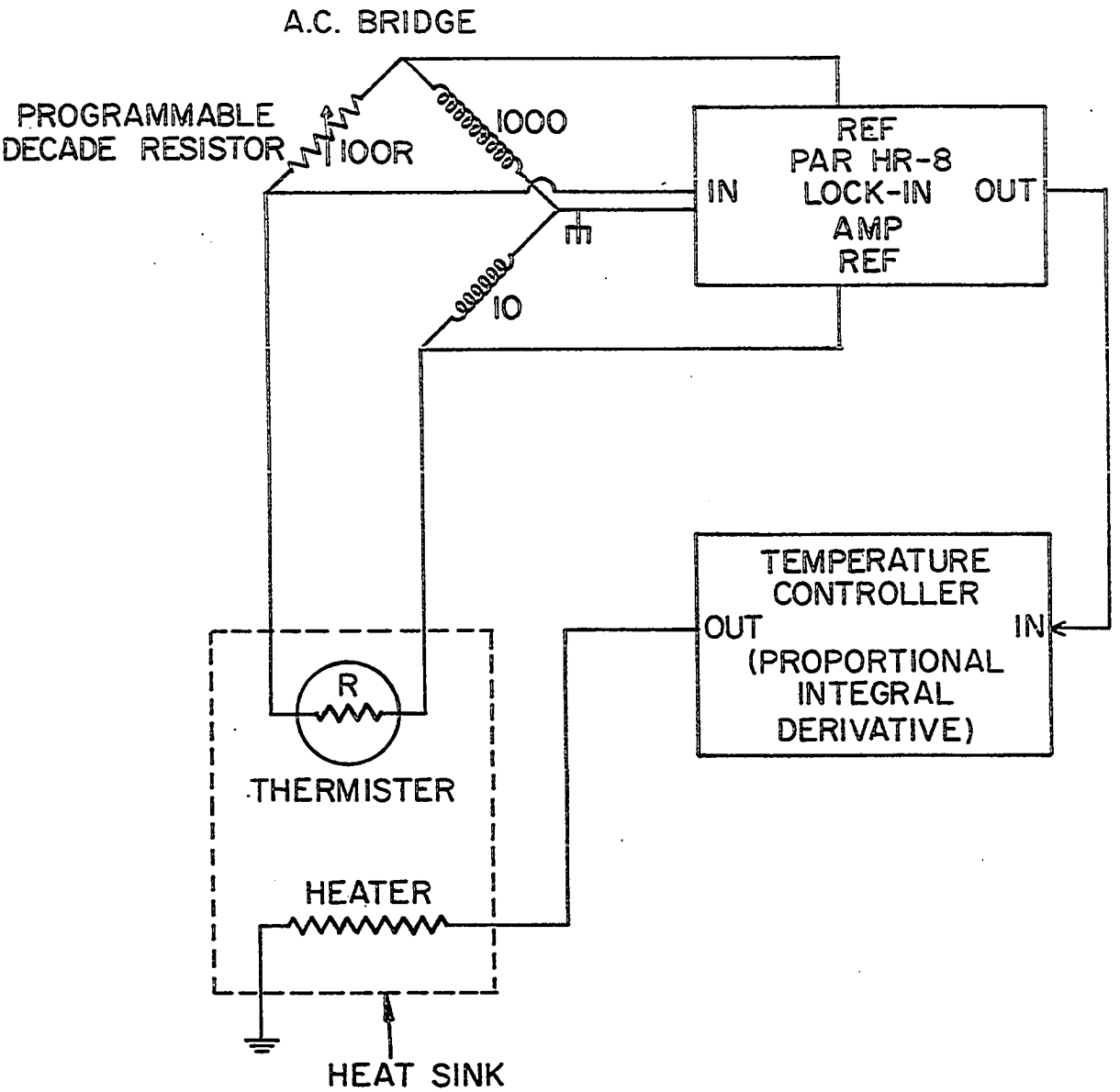

Figure 17. The flow chart of the BASIC program to control the experiment and record the data.

BASIC FLOW CHART

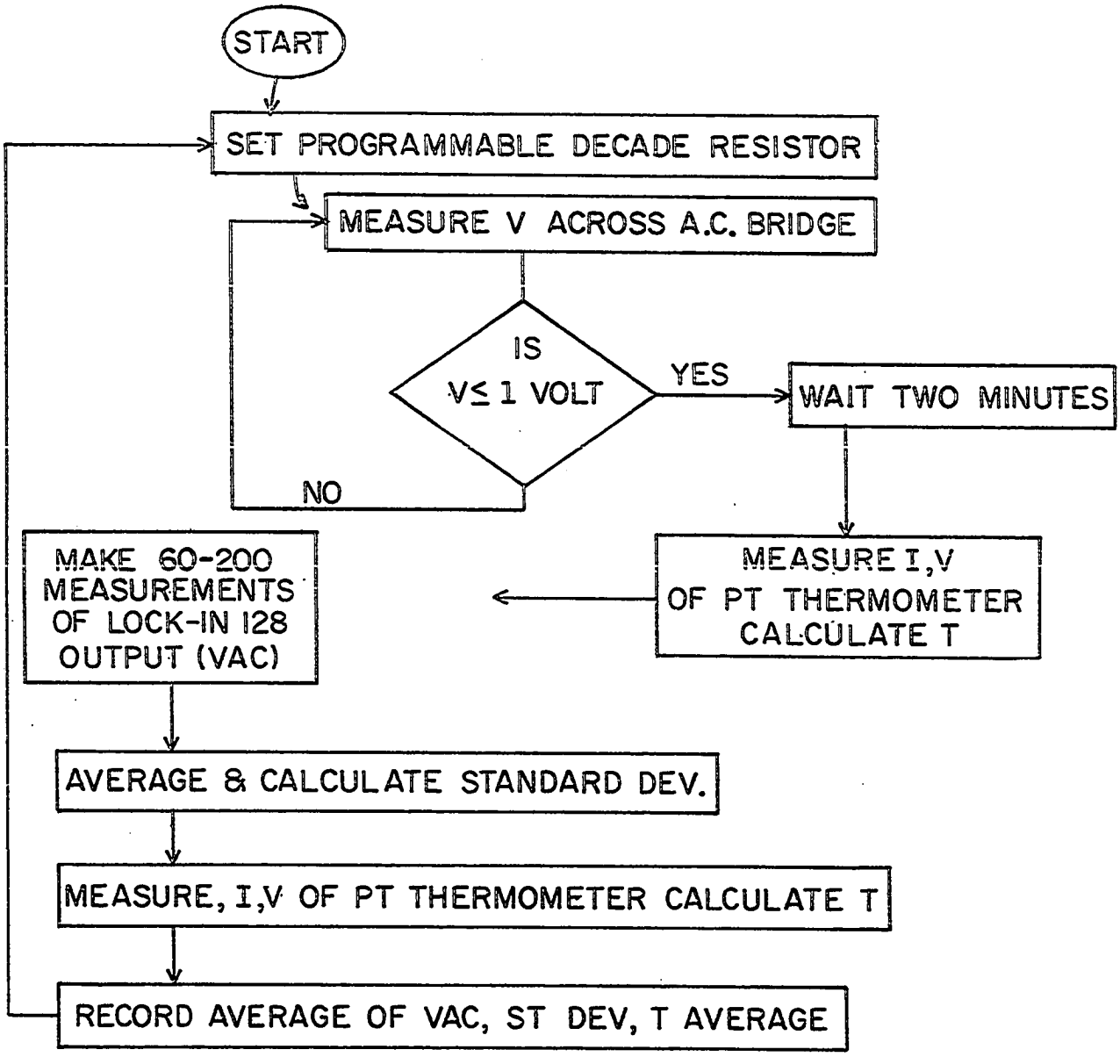

3.5 The Data Analysis

The heat capacity data is fit to the following equations:

$$C_p^+ = \frac{A^+}{\alpha}\left(|t|^{-\alpha} - 1\right) + B^+ + Dt \qquad (3.7)$$

$$C_p^- = \frac{A^-}{\alpha}\left(|t|^{-\alpha} - 1\right) + B^- + Dt \quad , \qquad (3.8)$$

where $t = (T-T_c)/T_c$ is reduced temperature. + refers to temperature above T_c and - to temperature below T_c. The fitting procedure assumes that both T_c and α are the same on both sides of the transition as expected for a critical point. The programs used are based on programs of Salamon and Lederman.[35] The data below T_c are interpolated so that for every point there is a point above T_c at the same absolute value of reduced temperature. The program then subtracts the linear background from the data points and does a linear least squares fit for C_p^+ as a function of C_p^-. The linear relationship between C_p^+ and C_p^- is based on the assumption that the exponent α is the same on both sides of the transition.

$$C_p^+ = \left(\frac{A^+}{A^-}\right) C_p^- + B^+ - (A^+B^-/A^-) \quad . \qquad (3.9)$$

The critical amplitude ratio A^+/A^-, which is the slope of the line, and $B^+-(B^- \times A^+/A^-)$, which is the intercept, are determined by the linear fit. Different values for the background slope, D, T_c, and the range of data fit are tried until the linear fit is optimized. The program calculates χ^2 for the linear fit and a linear correlation coefficient, which should approach 1. If the phase transition is not second order the assumption $\alpha^+ = \alpha^-$ will not hold, and a good linear fit cannot be obtained. The linear relationship between C_p^+ and C_p^- is used to merge the C_p^- data with C_p^+

data. A three parameter non-linear least squares fit, based on the technique called Marquadt's compromise,[36] is done on this merged set of data to find values for α, $A^{\pm}$, and B^{+}. χ^2 is calculated using the standard deviations measured for each data point. A^{-} and B^{-} are calculated from the slope and intercept resulting from the linear fit. Although it is not assumed that $B^{+} = B^{-}$ it has come out of the fitting procedure that they are the same, as theoretically predicted.[37]

The data analysis is done for different ranges of reduced temperature to find over what range the fitted parameters are not sensitive to range shrinking. Plots of log C' vs log t, where

$$C'^{+}(t) = \left[C^{+}_{data}(t) - (B^{+} + Dt - (A^{+}/\alpha))\right] \alpha/A^{+} \quad \text{and} \tag{3.10}$$

$$C'^{-}(t) = \left[C^{-}_{data}(t) - (B^{-} + Dt - (A^{-}/\alpha))\right] \alpha/A^{-} , \tag{3.11}$$

show where the experimental rounding occurs and indicate over what range the heat capacity obeys a power law. If the rounded region near T_c is included the value of α decreases. In the correct range of reduced temperature the parameters resulting from the fit are not sensitive to range shrinking.

The uncertainties in the exponent alpha are obtained by finding a 95% confidence range using the F-Test. For data in a given range of reduced temperature a plot is made of chi squared as a function of α, where each α is part of a parameter set including A^{+} and B^{+}, and the sets of parameters accepted are those for which

$$\left(\chi^2-\chi_o^2\right) / \chi_o^2 \leq \frac{p}{n-p} \left[F_{o,.05}(p,n-p)\right] \tag{3.12}$$

where p=3, the number of parameters fit, n = the number of data points, χ_o^2 is the minimum value of chi squared, and $F_{o,.05}$ is the 5% F distribution parameter. There is a 95% probability that the true value of A^+, α, and B^+ lie within the parameter space defined by the above equation.[38/]

CHAPTER 4

RESULTS AND DISCUSSION

4.1 Octyloxycyanobiphenyl Data and Chemical Analysis

The heat capacity data for the two samples of 80CB appear in Figure 18 where sample 1 is the earlier sample vacuum sublimated by Cladis. Two independent runs have been done on this sample, one at 1.96 Hz in August and the other at 9 Hz in December. The runs produce similar results for the background slope, alpha, and the critical amplitude ratio. The data for sample 1 in Figure 18 is from the December run on this sample. The rms value of the temperature oscillation is 5 mK. The heater power is on the order of 10^{-4} watts. Sample 2 in Figure 2 is the later sample. The rms temperature oscillation is 1-2 mK enabling us to fit the data closer to T_c. The frequency of the heater voltage is again 9 Hz and the power is on the order of 10^{-4} watts. The difference in the T_cs of the two samples is 32 mK ± 35 mK. This is the difference between the average T_c from the two runs on sample 1 and the T_c of sample 2. The transition temperatures are stable through repetitions of the experiment on each sample. The transition appears to be second order with a sharp symmetric peak for both samples within the experimental resolution. Neither flattening of the peak nor a two phase region is observed in either sample. No hysteresis between heating and cooling sweeps is observed. The transition may still be slightly first order but even in this case critical behavior is observed close to T_c.

Figure 18. The data on sample 1 is from the December run. The shapes of these curves illustrate the different behavior of these samples near the nematic-smectic A transition. In spite of the agreement between transition temperatures sample 1 produces $\alpha \simeq 0$ and sample 2's results show $\alpha \simeq .25$.

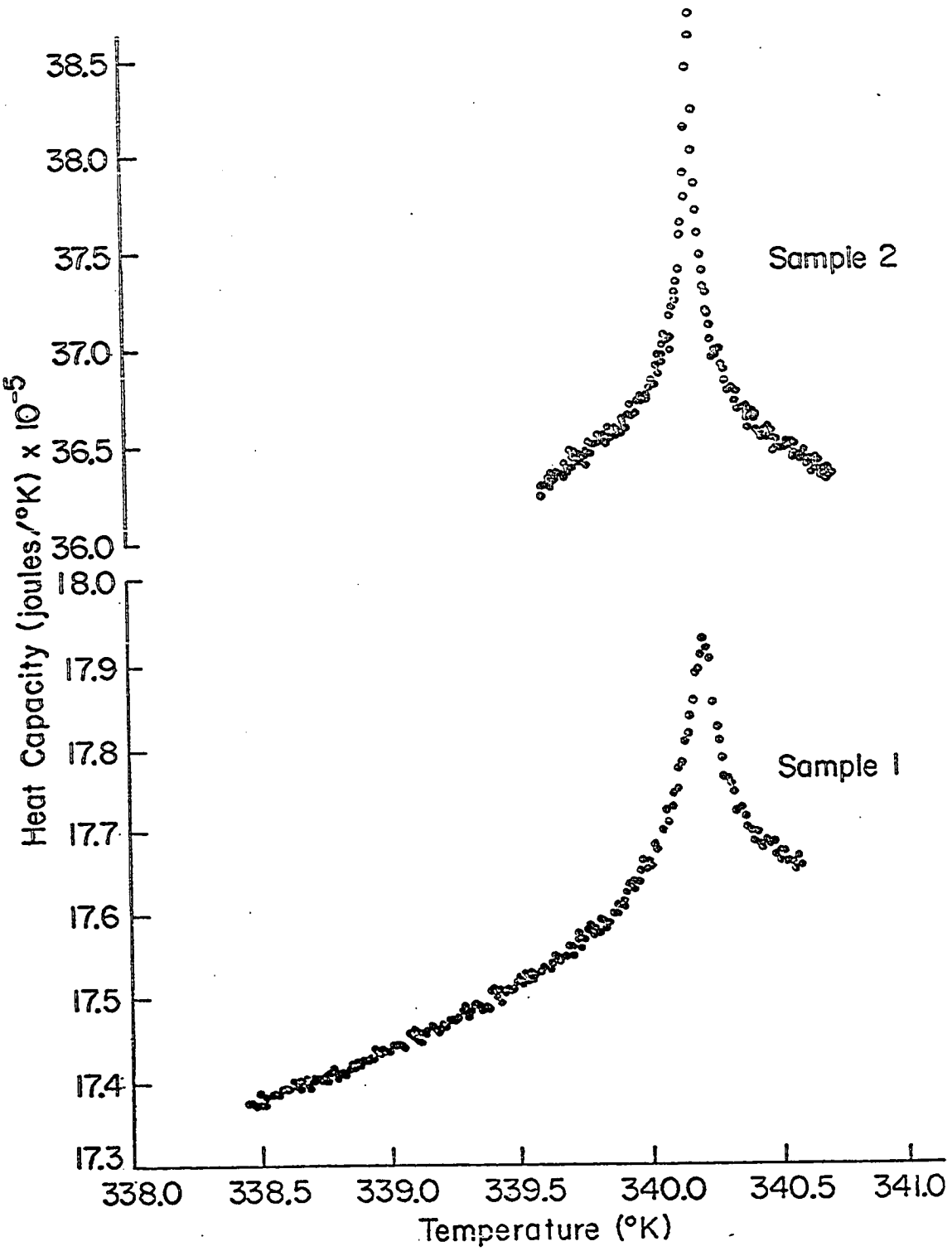

The values of alpha and other fitted parameters are listed in Table 2. More detailed tables of the results of fits on all the runs for different ranges of reduced temperature on the different samples appear in the Appendix. If data close to T_c are included, the value of alpha obtained from the fit is smaller due to experimental rounding. The range of data that should be fitted includes those points where the resulting fitted parameters are not sensitive to range shrinking. The log-log plots for the two samples of 80CB, shown in Figure 19, indicate the range of data where the heat capacity follows a power law and is not affected by rounding. The values shown in Table 2 are the results of fitting over a temperature range not affected by rounding and are those values which produce the best fits.

TABLE 2

SUMMARY OF RESULTS FOR SAMPLES OF 80CB

Sample	Range of $-\log\|t\|$	T_{dc}(mK)	T_{ac}(mK)	T_c(K)	α	A^+/A^-
1 - 8/79 run	2.3-4.2	154	10	340.107±3[a] mK, ±40[b] mK	.025±.04	1.39
1 - 12/79 "	2.9-4.0	---	5	340.215±7[a] mK, ±50[b] mK	.034±.03	1.3
2	2.9-4.6	100	1-2	340.193±2[a] mK, ±15[b] mK	.25 ±.02	1.2

[a] These errors are due to uncertainty in fitted value of T_c.

[b] These errors are due to uncertainty in dc temperature use.

The two different samples of 80CB measured are equivalent to those samples measured by Johnson[15] and Garland.[16] Johnson finds alpha ≤ zero in agreement with deGennes'[13] superconducting analogy and $A^+/A^- = 1.35$

Figure 19. Log-log plots for the two samples of 8OCB. The data for sample 1 where $\alpha \simeq 0$ rounds over further from T_c than the data for sample 2 where $\alpha \simeq .25$. Such plots indicate over which range of temperature the data can be analyzed without rounding affecting the exponent.

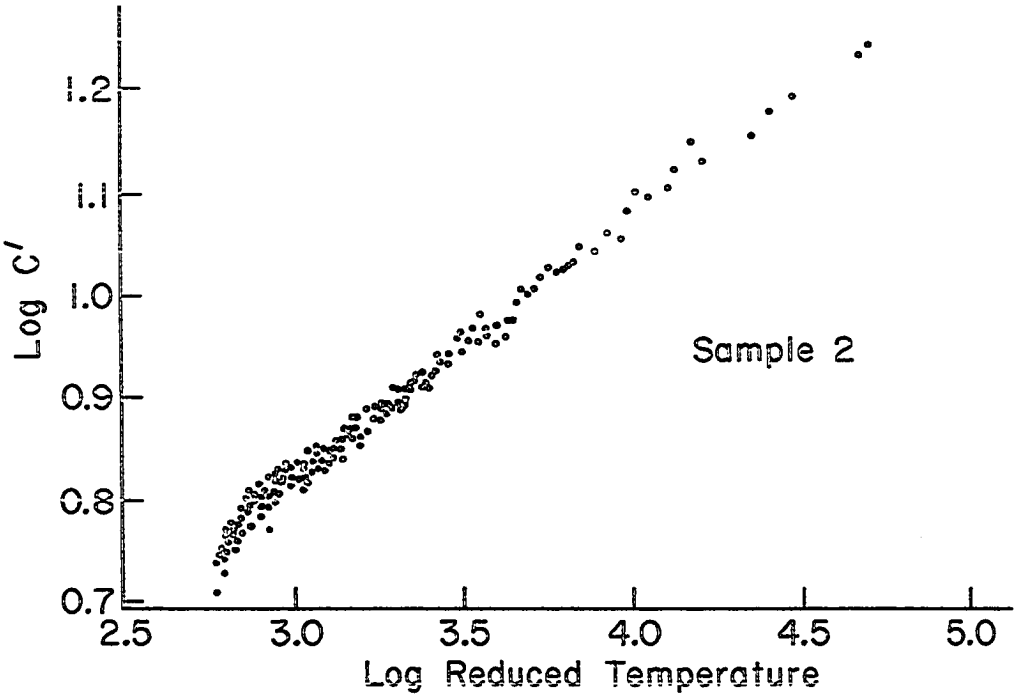

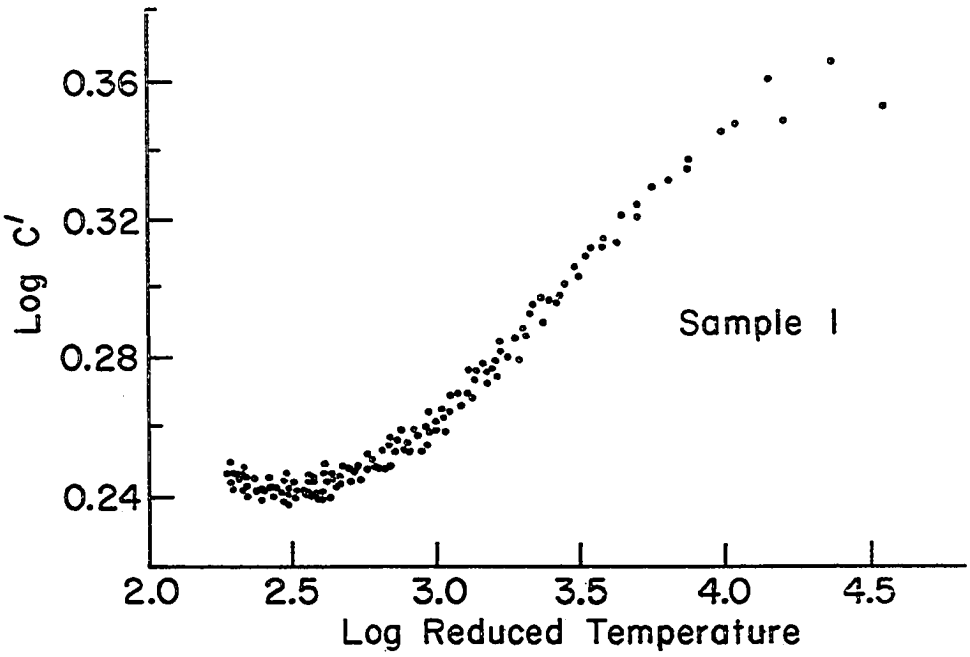

in a.c. heat capacity measurements on an early sample of 80CB. This agrees with the result for sample 1, the earlier sample shown in Table 2 ($\alpha = .03 \pm .03$, $A^+/A^- = 1.35$). Garland's measurements on a later batch of 80CB show alpha = $.25 \pm .05$ and $A^+/A^- = 1.0$. Sample 2 is from that same batch and yields $\alpha = .25 \pm .02$ and $A^+/A^- = 1.2$. The data from sample 1 cannot be fit to a power law with $\alpha = .25$ in any range of reduced temperature. Thus the lower exponent of sample 1 is not an artifact of experimental rounding due to impurities, but is indicative of different critical behavior.

The fact that the transition temperatures are in agreement is evidence that the two samples are the same compound. High pressure liquid chromatography[39] has shown that each sample has three overlapping peaks with a slight difference in the height of one of the peaks. This indicates the presence of impurities similar to the main compound; such as positional isomers. Homologous impurities may be ruled out as pure octylbromide would be used in the alkylation of the molecule. 220 MHz NMR has indicated the presence of only one component in each sample, although impurity levels on the order of 1% are difficult to detect with NMR British Drug Houses[40] reports a purity of greater than 99.9% for the later batch of 80CB where .01% impurities have been detected by gas liquid chromatography. The comparison of transition temperatures and chromatography data indicate that the samples are similar in composition. The information from British Drug Houses and the NMR data show that the level of impurities in each sample is less than a percent. The conclusion then is that the two samples of 80CB have small but differing concentrations of impurities which might be isomeric impurities.

4.2 Evidence for a Crossover Point

The fact that the two samples of 80CB behave so differently near the transition suggests that 80CB may be near a crossover point, such that a small change in composition places it in a different region of the phase diagram. Lubensky and Chen propose a crossover from anisotropic behavior to helium-like behavior followed by a tricritical point. Anisotropic behavior is characterized by $\nu_{||}$ and $\nu_{\perp}$ diverging at different rates as observed by Birgeneau.[17,18] Lubensky and Chen[1] predict that when K_1, the splay elastic constant, is very large, anisotropy results because splay is forbidden and the smectic layers cannot bend. As T_c is approached K_2 and K_3 are enhanced and when they are on the order of K_1 there is a crossover to isotropic helium-like behavior.

A critical point or second order transition is a fixed point unstable with respect to one variable such as temperature. A crossover point, however, is a fixed point which is unstable with respect to two variables. Exponents must be measured with respect to temperature and one other parameter to study a possible crossover.

The phase diagram for the nematic-smectic A transition may be studied by measuring alpha for several compounds where each compound has a different value of the Tna/Tni ratio. Table 3 shows results for all of the compounds studied including the value of Tna/Tni for each material. Detailed tables of results for different temperature ranges on different sets of data are shown in the Appendix for all of the samples. All of the measurements have been taken with temperature oscillations on the order of 1-5 mK. CBOOA and CBNOA were measured at f=9 Hz, 8CB at f=1.4 Hz, and $\overline{8}S5$ at 3.17 Hz. The results indicate two types of critical behavior with

TABLE 3

SUMMARY OF RESULTS

Sample	Tna/Tni	T_{ac}(mK)	T_c(K)	T_{dc}(mK)	-log|t| Range	α	A^+/A^-
CBNOA	.99	2-3	Heating 370.1±.1[b] Cooling 370.6±.1[b]	-------	-------	--------	----
8CB	.98	1	307.017±1[a]mK,±12[b]mK	53	2.6-4.0	.285±.03	.971
80CB (2)	.96	1-2	340.193±2[a]mK,±15[b]mK	100	2.9-4.6	.25 ±.02	1.2
80CB (1-8/79)	.96	10	340.107±3[a]mK,±40[b]mK	154	2.3-4.2	.025±.04	1.39
80CB (1-12/79)	.96	5	340.215±7[a]mK,±50[b]mK	-------	2.9-4.0	.034±.03	1.3
CBOOA	.94	3-4	356.950±1[a]mK	713	2.2-3.6	-.12 ±.02	.778
$\overline{8}$S5	.94	2-3	336.486±1[a]mK,±50[b]mK	$\lesssim$ 100	2.5-4.0	-.17 ±.03	.575

[a]Errors due to uncertainty in data fitting.

[b]Errors due to uncertainty in calculating dc temperature rise.

a crossover point at Tna/Tni=.96, the value corresponding to 80CB. Those compounds, whose ratio is below this value, have values of alpha less than or equal to zero. More rounding is observed around T_c so the data can not be fit as closely to T_c as with those runs where Tna/Tni $\geq$ .96. The linear fit is described by linear correlation coefficients which are typically around .98. The data for $\overline{8}$S5 and CBOOA appear in Figures 20 and 21. 8CB, whose Tna/Tni ratio is greater than .96, produces values of alpha around .3 and has a very sharp peak. The data, which is shown in Figure 22, can be analyzed to within several mK of T_c and the linear fits are characterized by linear correlation coefficients between .99 and 1.0. Clearly there are two types of critical behavior exhibited as a function of Tna/Tni, where the crossover occurs at Tna/Tni equal to .96.

CBNOA has Tna/Tni equal to .99 and exhibits a first order transition as evidenced by the .5° shift between the transition temperatures of the heating and cooling sweeps. This is illustrated in the data in Figure 23. There is also no pretransitional behavior observed, as there are no fluctuations characteristic of a critical point in CBNOA.

Summarizing these results, there are three regions of the phase diagram. Sample 1 of 80CB, $\overline{8}$S5, and CBOOA have rounded regions close to T_c and values of α near zero or negative. Sample 2 of 80CB and 8CB have sharp symmetric peaks with a large positive value of .3 for alpha. The crossover between these two types of critical behavior occurs at Tna/Tni=.96. CBNOA exhibits strong first order behavior. It appears that there is a tricritical point between Tna/Tni=.98, which is the value for 8CB, and Tna/Tni=.99, the value for CBNOA.

Figure 20. Heat capacity data for $\overline{8}S5$ where α equals $-.17 \pm .03$ and $A^+/A^- = .575$. Rounding appears at $-\log|t| = 3.6$. This is possibly a first order transition as the log-log plot shows $\alpha^+ \neq \alpha^-$ at $-\log|t| \simeq 3.6$.

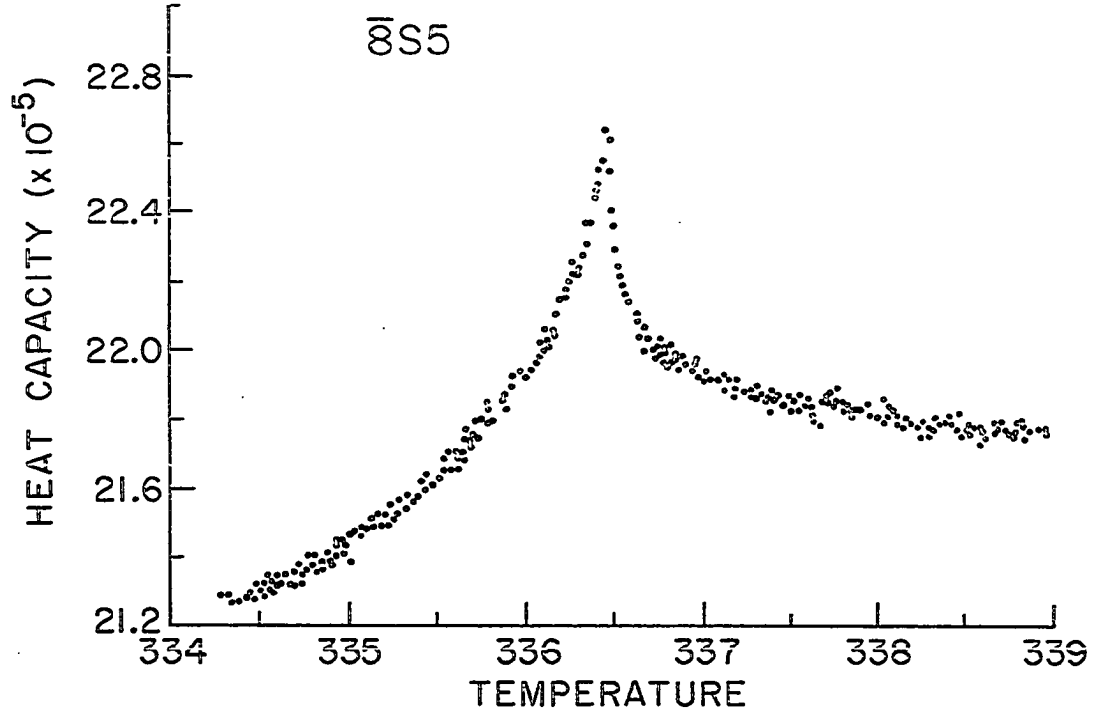

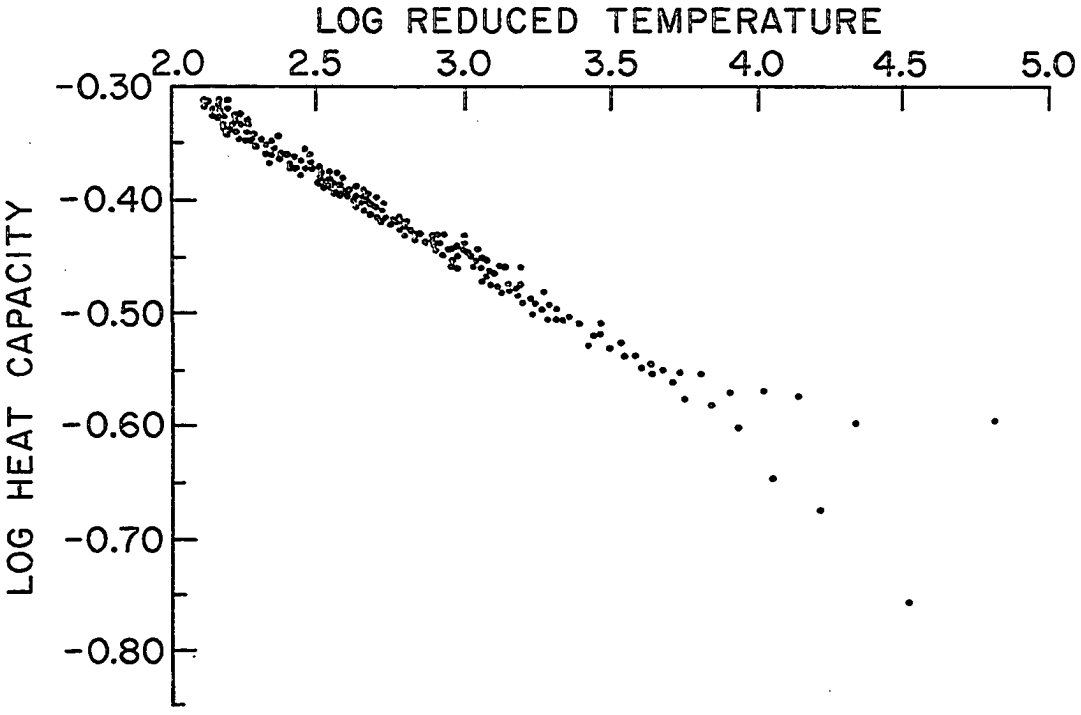

Figure 21. Heat capacity data for CBOOA where α = -.12 + .02 and A^+/A^- = .778. Rounding occurs at -log|t| = 3.7.

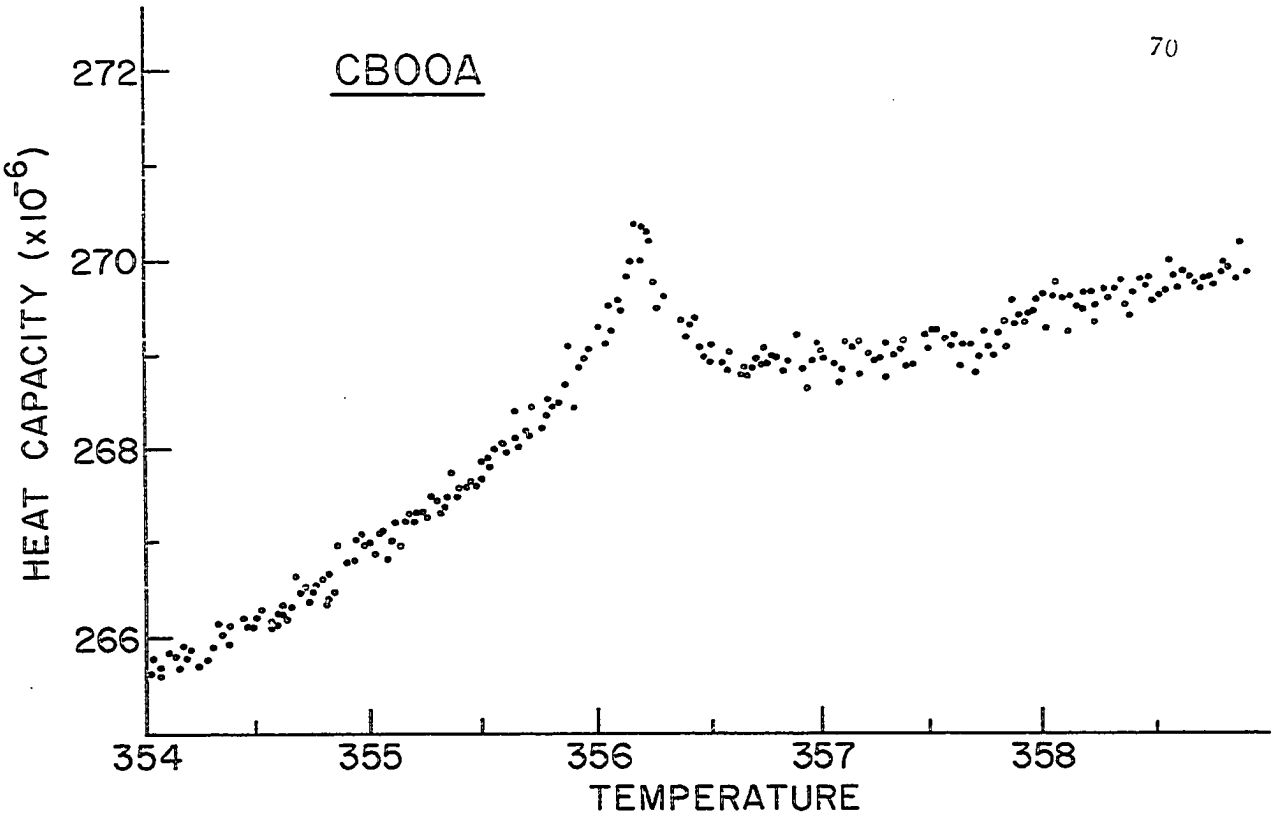

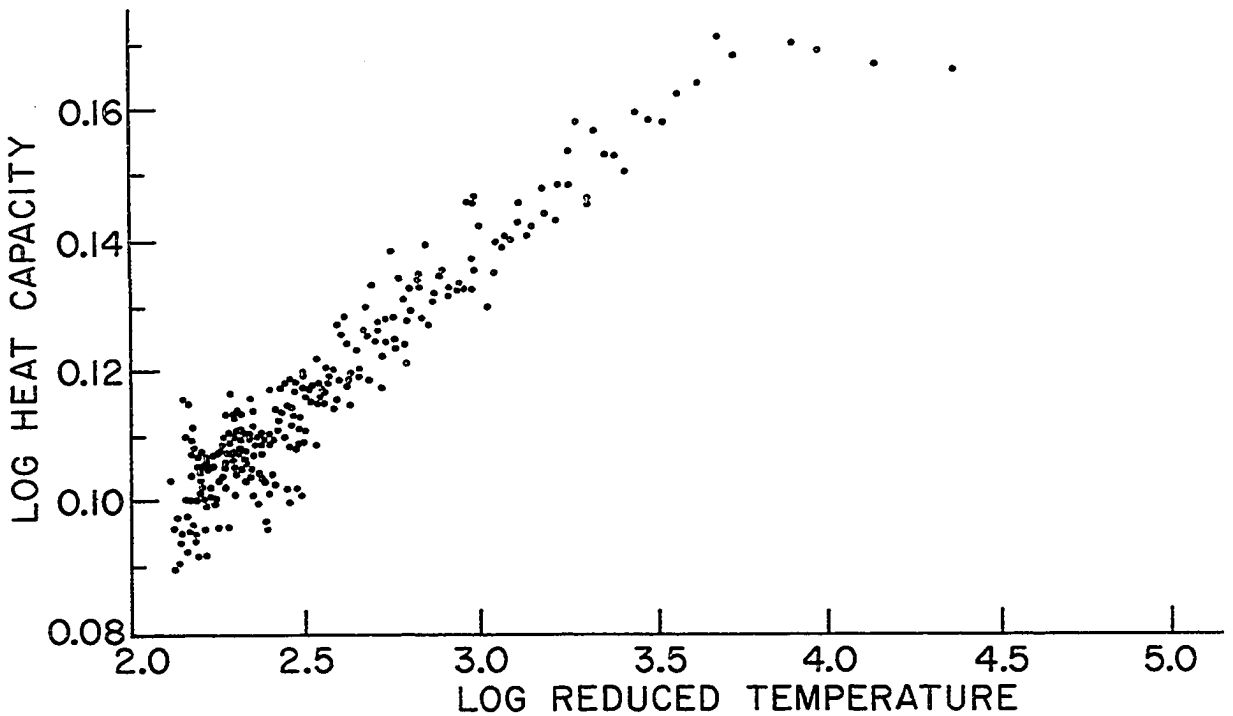

Figure 22. Heat capacity data for 8CB. The exponent α is .285±.03 and A^+/A^- = .971. Rounding appears at $-\log|t|$ = 4.5.

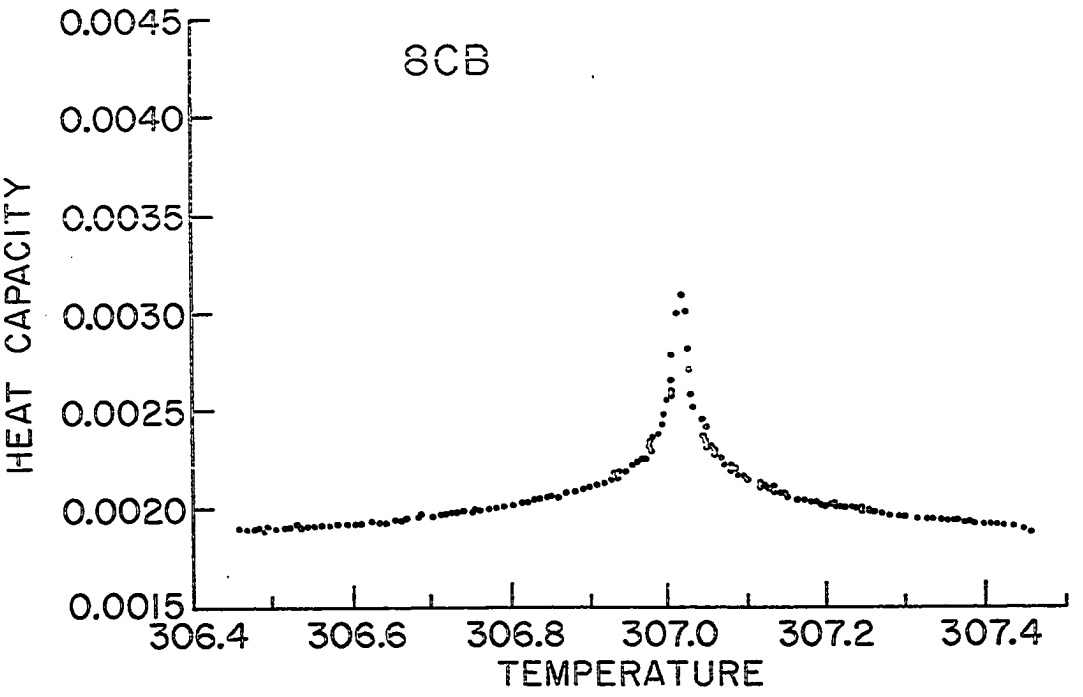

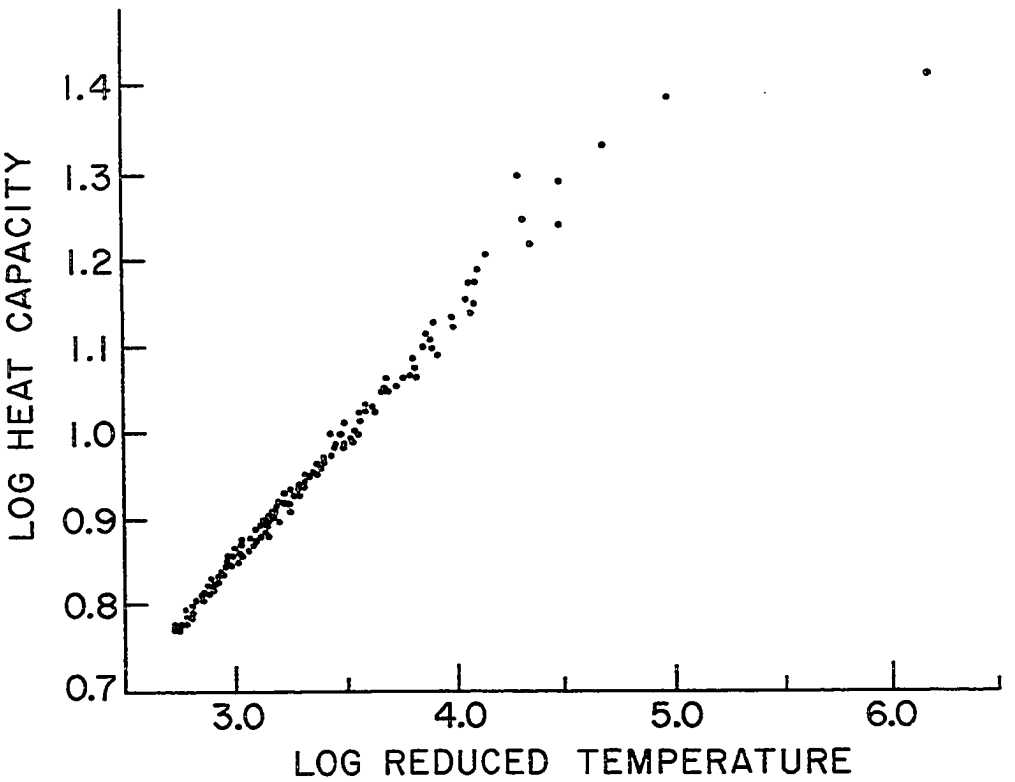

Figure 23. Heat capacity data for CBNOA showing the .5° shift in T_c between the heating and cooling sweeps. This hysteresis indicates a strong first order transition.

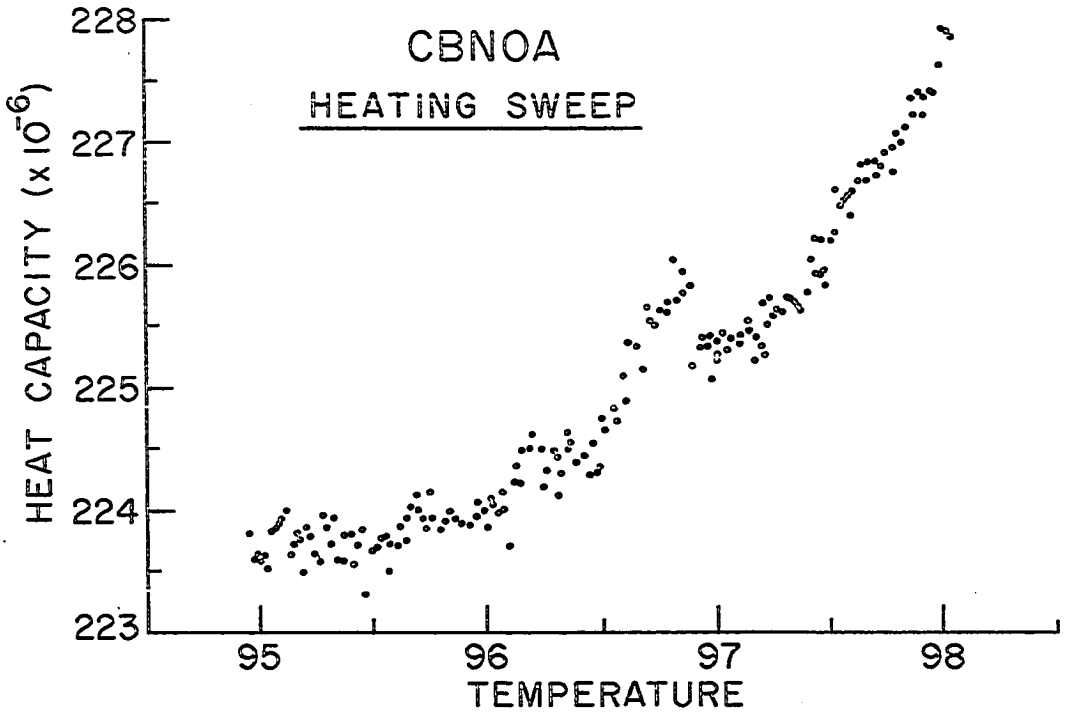

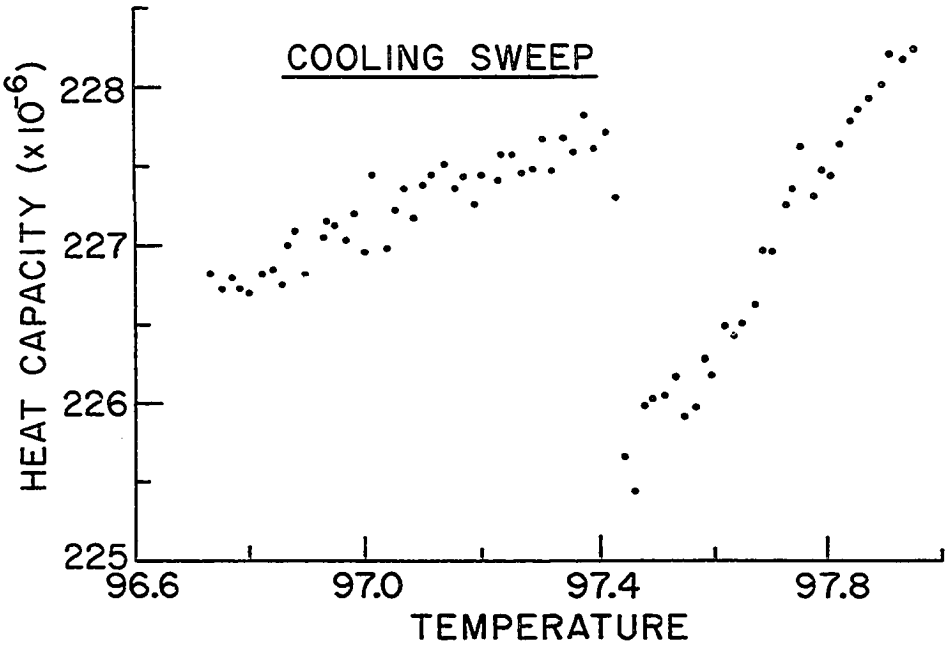

Garland[16] has done measurements of heat capacity on 80CB at high pressures where increased pressure produces a smaller value of Tna/Tni. At 500 bar, Tna=347.76, Tni=369.39, and Tna/Tni=.94 as compared with .96 at 1 bar. Garland observes a decrease in the amplitude of the peak at 500 bar and again at 1000 bar, but the exponent equals .25 at all pressures. This disagrees with the results in Table 3 which show lower exponents for CBOOA and $\overline{8}$S5, whose ratios are also .94. It also disagrees with Birgeneau's result for CBOOA that alpha equals .06 when $\nu_{||}$ and $\nu_{\perp}$ are substituted into the Josephson scaling law. A comparison with the alphas calculated from Birgeneau's measurements, however, may not be valid as the error bars on the alpha calculated from his x-ray results are large.

Brisbin et al.[41] have done heat capacity and birefringence measurements on three members of the $\overline{n}$S5 series and have obtained an indication of the crossover behavior exhibited by the data in Table 3. These results appear in Table 4, where the values of Tna/Tni are in the range .94-.99. Helium-like behavior is exhibited at Tna/Tni=.94. At Tna/Tni=.966 a crossover has occurred to quasicritical behavior with alpha = .25. At larger values of Tna/Tni there is a tricritical point. This is indicated by the tricritical value of .5 for alpha at Tna/Tni=.986 and the increasing hysteresis (T_C-T_C'). This sequence of behavior qualitatively agrees with the results in Table 3 and agrees with the prediction made by Lubensky and Chen[1] that there would be a crossover between two types of critical behavior as well as a tricritical point. The sequence of behavior predicted by Lubensky and Chen, anisotropic to helium-like to first order, however, does not agree with the experimental results.

TABLE 4

SUMMARY OF RESULTS OF BRISBIN ET AL.[41]

Compound	Tna/Tni	α	$T_c - T_c'$
$\overline{8}$S5	.94	0±.02	0±,007
$\overline{9}$S5	.97	.22±.03	.002±.01
$\overline{10}$S5	.986	.45±.05	.02 ±.01

4.3 Future Directions

The measurement of exponents would be more meaningful if better work were being done to determine whether the nematic-smectic A transition is first or second order. It has still not been resolved if this transition is always first order as predicted by Halperin, Lubensky, and Ma.[42] Although the assumption that $\alpha^+ = \alpha^-$ is valid even in slightly first order transitions, it would be interesting to follow the change in critical behavior as a function of the latent heat or of the size of the discontinuity in the order parameter. It is not clear whether the transitions observed in the compounds in Table 3 are purely second or slightly first order. Knowledge of this might explain why there is more rounding when the exponent is smaller. Brisbin et al.[41] incorporate birefringence measurements with high resolution specific heat measurements on the $\overline{n}$S5 series and observe a crossover point and a tricritical point. Similar measurements should be done on other series of compounds of exponents and of the order of the phase transition.

A complete physical picture of the nematic-smectic A transition will not emerge until there is agreement among different research groups on the

exponents and order of the transition for many compounds. Such repetition is necessary because of the difficulty of obtaining critical exponents on liquid crystals and the problems with chemical characterization. Better chemical analysis and purification techniques are important for more reliable measurements.

Another interesting possibility is to dope a pure liquid crystal, which is near the crossover point, such as 80CB, with controlled amounts of known impurity such as isomers or a neighboring homolog and attempt to shift the transition to the other side of the crossover point. The physical understanding of how a given impurity affects the ordering of the liquid crystal and its critical behavior would be important to the study of phase transitions in other systems. The region around the crossover point might also be explored by studying mixtures of two homologs and observing the exponent alpha as a function of concentration of one homolog in another. This would give a more detailed picture of the phase diagram around the crossover or tricritical point.

The motivation to understand the nematic-smectic A transition is that once it is understood an experimentally accessible system will exist where the effect of impurities on critical behavior and special crossover points can be studied in detail. The research presented in this thesis indicates that this transition may exhibit both a crossover point between two critical behaviors as well as a tricritical point and, therefore, may prove to be important to phase transition physics.

APPENDIX

This appendix contains detailed tables of the results of the fitting procedure on the different experiments on the different samples. The best fits are summarized in Chapter 4 and are those fits which are not affected by rounding and which fit the data without systematic deviations.

The error bars on T_c are expressed in two parts. The smaller uncertainty, a, is the uncertainty due to the fit while b is the uncertainty in T_c due to the uncertainty in the d.c. temperature rise.

8OCB SAMPLE 1 (8/79)

f (Hz)	T_{ac} (mK)	T_{dc} (K)	T_c (K)	D (J/K)	-log|t|	χ^2	A^+/A^-	A^+ (J/K)	B^+ (J/K)	A^- (J/K)	B^- (J/K)	α
1.96	10	.154	340.107 $\pm 3^a_{mk}, \pm 40^b_{mk}$	$.45\times10^{-3}$	2.9-4.2	.797	1.36	$.17\times10^{-5}$	$.167\times10^{-3}$	$.13\times10^{-5}$	$.171\times10^{-3}$	-.026
1.96	10	.154		$.45\times10^{-3}$		.810		$.88\times10^{-6}$	$.17\times10^{-3}$	$.65\times10^{-6}$	$.179\times10^{-3}$	.058
1.96	10	.154		$.45\times10^{-3}$		.807		$.94\times10^{-6}$	$.17\times10^{-3}$	$.69\times10^{-6}$	"	.05
1.96	10	.154		$.45\times10^{-3}$		.948		$.5\times10^{-5}$	$.157\times10^{-3}$	$.37\times10^{-5}$	$.164\times10^{-3}$	.165
1.96	10	.154		$.45\times10^{-3}$		.924		$.387\times10^{-6}$	$.193\times10^{-3}$	$.285\times10^{-6}$	$.176\times10^{-3}$	+.16
1.96	10	.154		$.45\times10^{-3}$		.833		$.26\times10^{-5}$	$.164\times10^{-3}$	$.191\times10^{-5}$	$.169\times10^{-3}$	-.08
1.96	10	.154		$.53\times10^{-3}$	2.3-5.0	1.82	1.36	$.177\times10^{-5}$	$.168\times10^{-3}$	$.130\times10^{-5}$	$.171\times10^{-3}$	-.05
						1.46		$.173\times10^{-5}$	$.168\times10^{-3}$	$.127\times10^{-5}$		-.05
						1.43		$.17\times10^{-5}$	$.168\times10^{-3}$	$.124\times10^{-5}$		-.054
						1.70		$.146\times10^{-5}$	$.169\times10^{-3}$	$.107\times10^{-5}$	$.172\times10^{-3}$	-.02
1.96	10	.154	340.107 $\pm 3^a_{mk}, \pm 40^b_{mk}$	$.35\times10^{-3}$	2.9-5.0	1.5	1.25	$.39\times10^{-5}$	$.161\times10^{-3}$	$.312\times10^{-5}$	$.165\times10^{-3}$	-.15
						3.8		$.565\times10^{-6}$	$.162\times10^{-3}$	$.452\times10^{-6}$	$.166\times10^{-3}$	.086
						1.8		$.217\times10^{-5}$	$.166\times10^{-3}$	$.174\times10^{-5}$	$.169\times10^{-3}$	-.073
						1.5		$.618\times10^{-5}$	$.155\times10^{-3}$	$.494\times10^{-5}$	$.160\times10^{-3}$	-.2
						2.5		$.302\times10^{-4}$	$.107\times10^{-3}$	$.242\times10^{-4}$	$.122\times10^{-3}$	-.4
				$.54\times10^{-3}$	2.9-4.2	1.54	1.39	$.134\times10^{-5}$	$.169\times10^{-3}$	$.969\times10^{-6}$	$.173\times10^{-3}$	-.005
						1.44		$.132\times10^{-5}$	$.169\times10^{-3}$	$.950\times10^{-6}$	"	-.0027
						1.227		$.137\times10^{-5}$	$.169\times10^{-3}$	$.986\times10^{-6}$	"	-.0076
						1.263		$.89\times10^{-6}$	$.17\times10^{-3}$	$.640\times10^{-6}$	"	.054
						1.6		$.399\times10^{-6}$	$.172\times10^{-3}$	$.287\times10^{-6}$	$.175\times10^{-3}$	.169
						1.23		$.12\times10^{-5}$	$.17\times10^{-3}$	$.863\times10^{-6}$	$.173\times10^{-3}$	.009
						2.15		$.8\times10^{-5}$	$.153\times10^{-3}$	$.576\times10^{-5}$	$.161\times10^{-4}$	-.276
						1.25		$.129\times10^{-5}$	$.169\times10^{-3}$	$.928\times10^{-6}$	$.173\times10^{-3}$	-.0002

80CB SAMPLE 1 (12/79)

f (Hz)	T_{ac} (mK)	T_{dc} (K)	T_c (K)	D (J/K)	-log|t|	χ^2	A^+/A^-	A^+ (J/K)	B^+ (J/K)	A^- (J/K)	B^- (J/K)	α
8.99	5	----	340.208 ±.003[a]	$.42\times10^{-3}$	2.9-4.6	16.9	1.34	$.117\times10^{-6}$	$.174\times10^{-3}$	$.823\times10^{-7}$	$.175\times10^{-3}$	.271
"	"	"	"	"	"	7.3	"	$.729\times10^{-6}$	$.17\times10^{-3}$	$.544\times10^{-6}$	$.172\times10^{-3}$	.06
"	"	"	"	"	"	7.1	"	$.8\times10^{-6}$	$.17\times10^{-3}$	$.597\times10^{-6}$	$.172\times10^{-3}$	.045
"	"	"	"	"	"	6.8	"	$.923\times10^{-6}$	$.169\times10^{-3}$	$.689\times10^{-6}$	$.171\times10^{-3}$	.028
"	"	"	"	"	"	6.7	"	$.992\times10^{-6}$	$.169\times10^{-3}$	$.741\times10^{-6}$	$.171\times10^{-3}$	.019
"	"	"	"	"	2.9-4.0	3.79	1.314	$.923\times10^{-6}$	$.169\times10^{-3}$	$.702\times10^{-6}$	$.171\times10^{-3}$	.034
"	"	"	"	"	"	3.81	"	$.937\times10^{-6}$	$.169\times10^{-3}$	$.713\times10^{-6}$	"	.032
"	"	----	340.223 ±.003[a]	$.26\times10^{-3}$	2.9-4.2	3.25	.862	$.807\times10^{-6}$	$.17\times10^{-3}$	$.936\times10^{-6}$	$.226\times10^{-3}$	.022
"	"	"	"	"	"	3.1	"	$.665\times10^{-6}$	$.171\times10^{-3}$	$.771\times10^{-6}$	$.227\times10^{-3}$	.046
"	"	"	"	"	"	3.01	"	$.537\times10^{-6}$	$.171\times10^{-3}$	$.623\times10^{-6}$	"	.073
"	"	"	"	"	"	3.03	"	$.57\times10^{-6}$	$.171\times10^{-3}$	$.661\times10^{-6}$	"	.066
"	"	"	"	$.47\times10^{-3}$	2.9-4.2	2.96	1.044	$.783\times10^{-6}$	$.17\times10^{-3}$	$.75\times10^{-6}$	$.171\times10^{-3}$	.037
"	"	"	"	"	"	2.87	"	$.62\times10^{-6}$	$.171\times10^{-3}$	$.594\times10^{-6}$	$.172\times10^{-3}$	.067
"	"	"	"	"	"	2.87	"	$.48\times10^{-6}$	$.171\times10^{-3}$	$.46\times10^{-6}$	"	.098
"	"	"	"	"	"	132.0	"	$.14\times10^{-6}$	$.172\times10^{-3}$	$.134\times10^{-6}$	$.173\times10^{-3}$	.295
"	"	"	"	"	"	2.85	"	$.53\times10^{-6}$	$.171\times10^{-3}$	$.51\times10^{-6}$	$.172\times10^{-3}$	.086
"	"	"	"	"	"	2.92	"	$.711\times10^{-6}$	$.170\times10^{-3}$	$.68\times10^{-6}$	$.171\times10^{-3}$	.049
"	"	----	"	$.47\times10^{-3}$	2.9-4.0	2.82	1.03	$.563\times10^{-6}$	$.171\times10^{-3}$	$.547\times10^{-6}$	$.172\times10^{-3}$	.078
"	"	"	"	"	"	2.88	"	$.718\times10^{-6}$	$.170\times10^{-3}$	$.697\times10^{-6}$	$.171\times10^{-3}$	.047
"	"	"	"	"	"	2.87	"	$.71\times10^{-6}$	$.170\times10^{-3}$	$.689\times10^{-6}$	$.171\times10^{-3}$	.048
"	"	"	"	"	"	3.65	"					-.077
"	"	"	"	"	"	2.94	"					.033

8OCB SAMPLE 2

f (Hz)	T_{ac} (mK)	T_{dc} (K)	T_c (K)	D (J/K)	-log|t|	χ^2	A^+/A^-	A^+ (J/K)	B^+ (J/K)	A^- (J/K)	B^- (J/K)	α
8.99	7	.385	340.209 ±.001[a],±.015[b]	$.95\times10^{-3}$	3.0-4.0	8.88	1.16	----	$.353\times10^{-3}$	----	$.359\times10^{-3}$	.256
"	"	"	"	"	"	8.85	"	$.636\times10^{-6}$	"	$.548\times10^{-6}$	"	.257
"	"	"	"	"	"	8.76	"	$.56\times10^{-6}$	$.354\times10^{-3}$	$.483\times10^{-6}$	$.355\times10^{-3}$	.272
"	"	"	"	"	"	18.53	"	$.337\times10^{-6}$	$.338\times10^{-3}$	$.291\times10^{-6}$	$.341\times10^{-3}$	.097
"	"	"	"	"	2.8-3.8	8.09	"	$.996\times10^{-6}$	$.35\times10^{-3}$	$.858\times10^{-6}$	$.354\times10^{-3}$	.198
"	"	"	"	"	"	7.65	"	$.726\times10^{-6}$	$.353\times10^{-3}$	$.626\times10^{-6}$	$.357\times10^{-3}$	.24
"	"	"	"	"	"	10.0	"	$.176\times10^{-5}$	$.346\times10^{-3}$	$.152\times10^{-5}$	$.351\times10^{-3}$	.123
"	"	"	"	"	2.6-3.6	7.88	1.18	$.115\times10^{-5}$	$.35\times10^{-3}$	$.975\times10^{-6}$	$.354\times10^{-3}$	.178
"	"	"	"	"	"	7.5	"	$.118\times10^{-5}$	$.35\times10^{-3}$	$.1\times10^{-5}$	"	.174
"	3-4	.179	"	$.998\times10^{-3}$	2.8-4.6	4.42	1.08	----	$.35\times10^{-3}$	----	$.352\times10^{-3}$	.181
"	"	"	"	"	"	4.22	"	$.104\times10^{-5}$	"	$.963\times10^{-6}$	"	.185
"	"	"	"	"	"	4.13	"	"	"	"	"	.186
"	"	"	"	"	"	3.7	"	$.1\times10^{-5}$	"	$.923\times10^{-6}$	"	.191
"	"	"	"	"	"	3.2	"	$.97\times10^{-6}$	"	$.899\times10^{-6}$	"	.194
"	1-2	.1	340.193 ±.001[a],±.015[b]	$.4\times10^{-3}$	2.4-5.0	2.67	1.2	$.107\times10^{-5}$	$.349\times10^{-3}$	$.892\times10^{-6}$	$.352\times10^{-3}$	.189
"	"	"	"	"	"	2.03	"	$.103\times10^{-5}$	$.35\times10^{-3}$	$.858\times10^{-6}$	$.353\times10^{-3}$	.194
"	"	"	"	"	"	2.02	"	$.101\times10^{-5}$	"	$.842\times10^{-6}$	"	.197
"	"	"	"	"	2.4-4.6	2.24	"	$.9\times10^{-6}$	"	$.75\times10^{-6}$	$.354\times10^{-3}$	.211
"	"	"	"	"	"	1.96	"	$.846\times10^{-6}$	"	$.71\times10^{-6}$	"	.219
"	"	"	"	"	"	1.69	"	$.617\times10^{-6}$	$.353\times10^{-3}$	$.514\times10^{-6}$	$.357\times10^{-3}$	.257
"	"	"	"	"	"	1.56	"	$.559\times10^{-6}$	$.353\times10^{-3}$	$.466\times10^{-6}$	$.357\times10^{-3}$	.271
"	"	"	"	"	2.4-4.4	1.9	"	$.589\times10^{-6}$	$.353\times10^{-3}$	$.49\times10^{-6}$	$.36\times10^{-6}$	.264
"	"	"	"	"	"	1.66	"	$.559\times10^{-6}$	"	$.466\times10^{-6}$	"	.27
"	"	"	"	"	"	1.58	"	$.81\times10^{-6}$	$.351\times10^{-3}$	$.675\times10^{-6}$	$.358\times10^{-3}$	.225
"	"	"	"	"	2.9-4.8	2.63	"	$.66\times10^{-6}$	$.353\times10^{-3}$	$.55\times10^{-6}$	$.359\times10^{-3}$	.245
"	"	"	"	"	"	2.14	"	$.85\times10^{-6}$	$.35\times10^{-3}$	$.71\times10^{-6}$	$.35\times10^{-3}$	.216
"	"	"	"	"	"	"	"	$.988\times10^{-6}$	"	$.82\times10^{-6}$	"	.199

f (Hz)	T_{ac} (mK)	T_{dc} (K)	T_c (K)	D (J/K)	-log|t|	χ^2	A^+/A^-	A^+ (J/K)	B^+ (J/K)	A^- (J/K)	B^- (J/K)	α
3.17	2-3	$\leq$.1	336.486 $\pm$.001[a], $\pm$.05[b]	$.3\times10^{-3}$	2.5-4.0	2.12	.575	$.495\times10^{-5}$	$.199\times10^{-3}$	$.861\times10^{-5}$	$.185\times10^{-3}$	-.156
"	"	"	"	"	"	2.14	"	$.475\times10^{-5}$	"	$.826\times10^{-5}$	"	-.149
"	"	"	"	"	"	2.08	"	----	$.197\times10^{-3}$	----	$.181\times10^{-3}$	-.178
"	"	"	"	"	"	2.67	"	----	$.205\times10^{-3}$	----	$.195\times10^{-3}$	-.06
"	"	"	"	"	2.2-3.6	2.26	.566	$.483\times10^{-5}$	$.199\times10^{-3}$	$.853\times10^{-5}$	$.185\times10^{-3}$	-.152

CBOOA

f (Hz)	T_{ac} (mK)	T_{dc} (K)	T_c (K)	D (J/K)	-log|t|	χ^2	A^+/A^-	A^+ (J/K)	B^+ (J/K)	A^- (J/K)	B^- (J/K)	α
8.97	3-4	206	356.096 ±.001[a]	$.35\times10^{-3}$	2.6-4.2	9.0	.744	$.125\times10^{-5}$	$.303\times10^{-3}$	$.168\times10^{-6}$	$.301\times10^{-3}$	-.22
"	"	"	"	"	"	9.2	"	$.272\times10^{-6}$	$.305\times10^{-3}$	$.366\times10^{-6}$	$.304\times10^{-3}$	.0065
"	"	"	"	"	"	9.2	"	$.178\times10^{-6}$	$.306\times10^{-3}$	$.239\times10^{-6}$	$.305\times10^{-3}$	.068
"	"	"	"	"	2.7-3.8	9.14	.742	$.44\times10^{-6}$	$.305\times10^{-3}$	$.593\times10^{-6}$	$.304\times10^{-3}$	-.069
"	"	"	"	"	"	9.17	"	$.412\times10^{-6}$	$.305\times10^{-3}$	$.555\times10^{-6}$	$.304\times10^{-3}$	-.059
"	"	"	"	"	"	9.19	"	$.27\times10^{-6}$	$.306\times10^{-3}$	$.364\times10^{-6}$	$.305\times10^{-3}$	.001
"	"	"	"	"	"	9.2	"	$.24\times10^{-6}$	$.306\times10^{-3}$	$.323\times10^{-6}$	"	.016
"	"	"	"	"	"	9.19	"	$.257\times10^{-6}$	$.306\times10^{-3}$	$.346\times10^{-6}$	"	,0075
"	"	"	"	"	"	9.23	"	$.376\times10^{-6}$	$.305\times10^{-3}$	$.507\times10^{-6}$	$.304\times10^{-3}$	-.047
8.97	3-4	161	356.099 ±.001[a]	$.35\times10^{-3}$	2.6-4.0	6.45	.870	$.3\times10^{-6}$	$.307\times10^{-3}$	$.35\times10^{-6}$	$.306\times10^{-3}$	.05
"	"	"	"	"	"	7.55	"	$.1\times10^{-6}$	$.308\times10^{-3}$	$.11\times10^{-6}$	$.401\times10^{-3}$	.195
"	"	"	"	"	"	6.26	"	$.108\times10^{-5}$	$.305\times10^{-3}$	$.12\times10^{-5}$	$.304\times10^{-3}$	-.124
"	"	"	"	"	"	6.65	"	$.7\times10^{-6}$	$.306\times10^{-3}$	$.80\times10^{-6}$	$.305\times10^{-3}$	-.066
"	"	"	"	"	"	7.1	"	$.456\times10^{-6}$	$.307\times10^{-3}$	$.524\times10^{-6}$	$.306\times10^{-3}$	-.005
"	"	"	"	"	2.6-3.7	6.79	.763	$.366\times10^{-6}$	$.307\times10^{-3}$	$.48\times10^{-6}$	$.306\times10^{-3}$	.023
"	"	"	"	"	"	7.5	"	$.158\times10^{-6}$	$.308\times10^{-3}$	$.207\times10^{-6}$	$.307\times10^{-3}$	.140
"	"	"	"	"	"	8.0	"	$.215\times10^{-6}$	$.308\times10^{-3}$	$.282\times10^{-6}$	"	.097
"	"	"	"	"	"	7.6	"	$.911\times10^{-6}$	$.306\times10^{-3}$	$.119\times10^{-5}$	$.305\times10^{-3}$	-.108

CBOOA (continued)

f (Hz)	T_{ac} (mK)	T_{dc} (K)	T_c (K)	D (J/K)	-log|t|	χ^2	A^+/A^-	A^+ (J/K)	B^+ (J/K)	A^- (J/K)	B^- (J/K)	α
8.97	3-4	713	356.950 ±.001[a]	$.35\times10^{-3}$	2.2-4.0	7.8	.786	$.292\times10^{-5}$	$.259\times10^{-3}$	$.369\times10^{-5}$	$.257\times10^{-3}$	-.26
"	"	"	"	"	2.5-3.8	7.8	.719	$.906\times10^{-6}$	$.264\times10^{-3}$	$.126\times10^{-5}$	$.263\times10^{-3}$	-.077
"	"	"	"	"	"	4.7	"	$.166\times10^{-5}$	$.262\times10^{-3}$	$.231\times10^{-5}$	$.260\times10^{-3}$	-.159
"	"	"	"	"	2.2-3.6	4.76	.778	$.124\times10^{-5}$	$.263\times10^{-3}$	$.159\times10^{-5}$	$.262\times10^{-3}$	-.124
"	"	"	"	"	"	5.6	"	$.428\times10^{-6}$	$.265\times10^{-3}$	$.550\times10^{-6}$	$.265\times10^{-3}$	.045
"	"	"	"	"	"	7.2	"	$.458\times10^{-6}$	$.265\times10^{-3}$	$.589\times10^{-6}$	"	.033
"	"	"	"	"	"	9.5	"	$.375\times10^{-6}$	$.265\times10^{-3}$	$.482\times10^{-6}$	"	.064
"	"	"	"	"	"	12.7	"	$.472\times10^{-6}$	$.265\times10^{-3}$	$.607\times10^{-6}$	"	.029
8.97	5-6	1,210	356.95 ±.001[a]	$.33\times10^{-3}$	2.3-3.7	5.88	1.213	$.203\times10^{-5}$	$.288\times10^{-3}$	$.167\times10^{-5}$	$.29\times10^{-3}$	-.109
"	"	"	"	"	"	6.24	"	$.144\times10^{-5}$	$.29\times10^{-3}$	$.119\times10^{-5}$	$.292\times10^{-3}$	-.057
"	"	"	"	"	"	14.54	"	$.133\times10^{-6}$	$.295\times10^{-3}$	$.110\times10^{-6}$	$.296\times10^{-3}$	.299
"	"	"	"	"	2.4-3.5	5.05	1.13	$.974\times10^{-6}$	$.292\times10^{-3}$	$.862\times10^{-6}$	$.293\times10^{-3}$	-.0067
"	"	"	"	"	"	5.09	"	$.98\times10^{-6}$	$.29\times10^{-3}$	$.867\times10^{-6}$	$.291\times10^{-3}$	-.008
"	"	"	"	"	"	4.99	"	$.15\times10^{-5}$	$.29\times10^{-3}$	$.133\times10^{-5}$	"	-.07
"	"	"	"	"	2.4-3.4	5.18	1.12	$.948\times10^{-6}$	$.292\times10^{-3}$	$.846\times10^{-6}$	$.292\times10^{-3}$	-.002

f (Hz)	T_{ac} (mK)	T_{dc} (K)	T_c (K)	D (J/K)	-log|t|	χ^2	A^+/A^-	A^+ (J/K)	B^+ (J/K)	A^- (J/K)	B^- (J/K)	α
1.43	1	.053	307.017 ±.001[a],±.012[b]	$.5\times10^{-2}$	2.6-4.2	7.29	.963	$.127\times10^{-4}$	$.161\times10^{-2}$	$.132\times10^{-4}$	$.163\times10^{-2}$	.325
"	"	"	"	"	"	7.55	"	$.162\times10^{-4}$	$.158\times10^{-2}$	$.168\times10^{-4}$	$.160\times10^{-2}$	.295
"	"	"	"	"	"	7.79	"	$.204\times10^{-4}$	$.154\times10^{-2}$	$.212\times10^{-4}$	$.156\times10^{-2}$	.267
"	"	"	"	"	"	8.0	"	----	$.154\times10^{-2}$	----	$.159\times10^{-2}$	.289
"	"	"	"	"	2.6-4.0	4.96	.971	$.166\times10^{-4}$	$.158\times10^{-2}$	$.171\times10^{-4}$	$.16\times10^{-2}$	.291
"	"	"	"	"	"	4.92	"	$.179\times10^{-4}$	$.157\times10^{-2}$	$.179\times10^{-4}$	$.159\times10^{-2}$	.284
"	"	"	"	"	"	4.99	"	----	----	----	----	.268
"	3	.101	307.016 ±001[a],±.012[b]	"	2.6-4.2	12.18	1.13	$.147\times10^{-5}$	$.37\times10^{-3}$	$.131\times10^{-5}$	$.39\times10^{-3}$	.424
"	"	"	"	"	"	17.75	"	$.101\times10^{-5}$	$.378\times10^{-3}$	$.894\times10^{-6}$	$.397\times10^{-3}$	.471
"	"	"	"	"	"	15.8	1.13	$.139\times10^{-5}$	$.371\times10^{-3}$	$.123\times10^{-5}$	$.391\times10^{-3}$	.431
"	"	"	"	"	2.6-4.5	20.0	1.13	$.177\times10^{-5}$	$.365\times10^{-3}$	$.157\times10^{-5}$	$.383\times10^{-3}$	.4
"	"	"	"	"	"	19.5	"	$.123\times10^{-5}$	$.374\times10^{-3}$	$.109\times10^{-5}$	$.391\times10^{-3}$	.45
"	"	"	"	"	"	20.74	"	$.126\times10^{-5}$	$.373\times10^{-3}$	$.112\times10^{-5}$	$.39\times10^{-3}$	.44
"	"	"	"	"	3.0-4.0	8.5	"	$.143\times10^{-5}$	$.37\times10^{-3}$	$.127\times10^{-5}$	$.388\times10^{-3}$	.421
"	"	"	"	"	"	11.9	"	$.242\times10^{-5}$	$.356\times10^{-3}$	$.214\times10^{-5}$	$.375\times10^{-3}$	.361
"	"	"	"	"	"	13.0	"	$.147\times10^{-5}$	$.37\times10^{-3}$	$.13\times10^{-5}$	$.388\times10^{-3}$	.422
"	"	"	"	"	"	12.3	"	$.181\times10^{-5}$	$.365\times10^{-3}$	$.16\times10^{-5}$	$.384\times10^{-3}$	.397

REFERENCES

1. Lubensky, T. C. and Chen, J., Phys. Rev. B 17, 366 (1978).

2. Van der Meer, B. W., "Molecular Models for Cholesteric and Smectic Liquid Crystals," Ph.D. Thesis, University of Groningen, 1979.

3. McMillan, W. L., Phys. Rev. A 4, 1238 (1971).

4. Kobayashi, K. K., J. Phys. Soc. Japan 29, 101 (1970).

5. Alben, R., Solid State Communications 13, 1783 (1973).

6. Flick, C. and Doane, J. W., Phys. Lett. A 47, 331 (1974).
Johnson, D. L., Maze, C., Oppenheim, E., and Reynolds, R., Phys. Rev. Lett. 34, 1143 (1975).
Hardouin, F., Sigaud, G., Achard, M. F., Gasparoux, H., Solid State Communications 22, 343 (1977).

7. McMillan, W. L. Phys. Rev. A 7, 1419 (1973).

8. Cabane, B. and Clark, W. G., Solid State Communications 13, 129 (1973).

9. Cladis, P. E. and Torza, S., Phys. Rev. Lett. 32, 1406 (1974).

10. Djurek, D., Baturic-Rubcic J., and Franulovic, K. Phys. Rev. Lett. 33, 1126 (1974).

11. deGennes, P. G., The Physics of Liquid Crystals, Oxford University Press, Belfast, (1974).

12. McMillan, W. L., Phys. Rev. A 6, 936 (1972).

13. deGennes, P. G., Solid State Communications 10, 753 (1972).

14. Schantz, C. A. and Johnson, D. L., Phys. Rev. A 17, 1504 (1978).

15. Johnson, D. L., Hayes, C. F., deHoff, R. J., and Schantz, C. A., Phys. Rev. B 18, 4902 (1978).

16. Garland, Carl W., Kasting, Gerald, B., and Lushington, Kenneth J., Phys. Rev. Lett. 43, 1420 (1979).

17. Davidov, D., Safinya, C. R., Kaplan, M., Schaetying, R. Birgeneau, R. J., and Litster, J. D., Phys. Rev. B 19, 1657 (1979).

18. Litster, J. D., Birgeneau, R. J., Kaplan, M., Safinya, C. R., and Als-Neilsen, J. in "Ordering in Strongly Fluctuating Condensed Matter Systems," Proceedings of the NATO Advanced Study Institute, April, 1979, Geilo, Norway, edited by T. Riste, C. Plenum, New York, to be published.

19. The usual version of the Josephson scaling law is: $\frac{2-\alpha}{d} = \nu$.

20. Smaardyk, J. E., unpublished Ph.D. thesis, University of Illinois, Urbana-Champaign (1975).

21. Smaardyk, J. E., and Mochel, J. M., Review of Scientific Instruments 49, 988 (1978).

22. Sullivan, P. and Seidel, G., Phys. Rev. 173, 679 (1968).

23. Stycast 1266 is made by Emerson and Cuming, Inc., Northbrook, Illinois. The resin is mixed with 28% of catalyst by weight and cured for several hours at 100 C.

24. Mylar is a registered trademark of E. I. DuPont de Nemours and Co., Inc., Wilmington, Deleware, which is used for a polyester film that they manufacture.

25. Chromel A is a registered trademark of Hoskins Manufacturing Co., Detroit, Michigan, which is used for a nickel-chromium wire that they manufacture.

26. Torr Seal is a registered trademark of Varian in Palo Alto, California, and is a low vapor pressure epoxy made by mixing equal lengths of resin and hardener. It is cured at room temperature in 30 minutes.

27. Epo-Tek 417 is a two component, electrically conductive epoxy containing pure silver; 1/15 parts by weight of hardener is added to the silver base and the epoxy is cured for two hours at 80° C. Epo-Tek 417 is made by Epoxy Technology, Inc., in Billerica, MA.

28. Silicone O-rings were obtained from Buckeye Rubber & Packing Company of Cleveland, Ohio.

29. LeGrange, J. D., Mochel, J. M., "High Resolution Heat Capacity Studies Near the Nematic-Smectic A Transition in 80CB," to appear in Physical Review Letters.

30. British Drug Houses Chemicals Ltd., Poole, England.

31. Eastman Organic Chemicals, Eastman Kodak Co., Rochester, New York.

32. PET is a trademark of Commodore Business Machines in Palo Alto, California, and is a microcomputer with 8K of memory based on the Motorola 6502 chip.

33. Sauereisen cement is manufactured by Sauereisen Cements Co., Pittsburgh, PA.

34. Platinum thermometers were obtained with calibrations from Rosemount Inc., in Minneapolis.

35. Lederman, F. L., unpublished Ph.D. Thesis, University of Illinois, Urbana-Champaign (1975).

36. Bevington, P. R., Data Reduction and Error Analysis for the Physical Sciences, McGraw-Hill, New York, 1969.

37. Barmatz, M., Hohenberg, R. C., Kornblit, A., Phys. Rev. B 12, 1947 (1975).

38. Lipa, J. A., Edwards, O., Buckingham, M. J., Phys. Rev. A 15, 778 (1977).

39. A Regis #731003 spherisorb Amino column was used with .125% isopropyl alcohol in hexane as the solvent. A 5 micron spherisorb silica column also showed multiple overlapping peaks.

40. This information was obtained from letters exchanged with Dr. B. Sturgeon of BDH Chemicals Ltd., Poole, Dorset BH124NN, United Kingdom.

41. Brisbin, D., DeHoff, R., Lockhart, T. E., and Johnson, D. L., Phys. Rev. Lett. 43, 1171 (1979).

42. Halperin, B. F., Lubensky, T. C., and Ma, S.-K., Phys. Rev. Lett. 32, 292 (1979).

VITA

Jane Deborah LeGrange was born in New York City on September 21, 1953. She attended public schools on Long Island. She received a Bachelor's degree cum laude from the University of Pennsylvania in May, 1975. As an undergraduate she participated in research projects at University of Pennsylvania, Yale University, and Weizmann Institute. She entered graduate school at the University of Illinois in August, 1975, and received the M.S. degree in physics in February, 1977. She is currently a member of the American Physical Society.